Summary of Professional Accomplishments

1. Name: Katarzyna KRUPA

2. Diplomas, degrees conferred in specific areas of science or arts, including the name of the institution which conferred the degree, year of degree conferment, title of the PhD dissertation

- **PhD degree in Technical Sciences** in scope of Machine Design and Maintenance, conferred by Scientific Council of the Faculty of Mechatronics of the Warsaw University of Technology on 20th January 2010

  PhD in Engineering Sciences, conferred by the University of Besançon on 14th December 2009

  Title of PhD dissertation: "Optonumerical analysis of AlN piezoelectric thin film operating as an actuation layer in micro-cantilevers"

  PhD prepared in the framework of the *co-tutelle* international agreement between the Warsaw University of Technology (Poland) and the University of Besançon (France)

- **MSc Engineering** obtained in Automatic Control and Robotics in scope of Photonics Engineering at the Faculty of Mechatronics of the Warsaw University of Technology on 19th September 2004

  Title of MSc dissertation: "Development of phase correction algorithm for implementation in Fourier Transform Spectrometry"

3. Information on employment in research institutes or faculties/departments or school of arts

From 01/2024	Assistant Professor Institute of Physical Chemistry Polish Academy of Sciences, Warsaw, Poland
12/2019 – 12/2023	Assistant Professor Institute of Physical Chemistry Polish Academy of Sciences, Warsaw, Poland Junior group leader in the TEAM-NET project of the Foundation for Polish Science (POIR.04.04.00-00-16ED/18-00)
12/2018 – 11/2019	Post-doctoral researcher Université Bourgogne Franche-Comté, Laboratoire Interdisciplinaire Carnot de Bourgogne (ICB), UMR CNRS* 6303, Dijon, France Post-doc in the ISITE-BFC of the French National Research Agency ANR** (ANR-15-IDEX-0003-MIRCOMB)
06/2017 – 10/2018	Post-doctoral researcher

* CNRS (« Centre National de la Recherche Scientifique ») – French National Center of the Scientific Recherche

** ANR (« Agence National de la Recherche ») – French National Research Agency

	Università degli Studi di Brescia, Dipartimento di Ingegneria dell'Informazione, Brescia, Italy
	10/2017 – 10/2018: Post-doc Fellow of European Marie Sklodowska-Curie COFUND grant (H2020 MSCA-COFUND Multiply, No.713694)
	06/2017 – 09/2017: Post-doc in ERC Advanced Grant (No. 740355)
04/2016 – 04/2017	Post-doctoral researcher
	Université Bourgogne Franche-Comté, Laboratoire Interdisciplinaire Carnot de Bourgogne (ICB), UMR CNRS* 6303, Dijon, France
	Post-doc in the project of the Indo-French Center for the promotion of Advanced Research (IFCPAR) (IFC/2/4052-EPD/5104-2/2016/146)
10/2010 – 12/2015	Post-doctoral researcher
	Université de Limoges, Institut XLIM, Département Photonique, UMR CNRS* 7252, Limoges, France
	Post-doc in the two projects of the French National Research Agency ANR** (ANR 08-JCJC-0122 PARADHOQS and ANR Labex SIGMA-LIM grant no. VIP2013) and in one collaborative R&D project under OSEO-ISI programme (DAT@DIAG)

4. Description of the achievements, set out in art. 219 para 1 point 2 of the Act

My research work, performed after receiving my PhD, has significantly contributed to the field of multimode nonlinear fiber optics that over the last more than 10 years has experienced a strong resurgent of interest. My keynote discoveries, that further opened new directions in the field, are related to the original spatiotemporal dynamics based on collective evolutions of light beams. Namely, I have demonstrated experimentally an efficient frequency conversion in a graded-index multimode fiber through an effect called geometric parametric instability (GPI), induced by the natural oscillations along the fiber of a narrowband multimode beam (*K. Krupa et al., PRL 116, 183901, 2016; 184 citations without self-citations from Scopus*). These results have permitted for the remarkable possibility to convert a near-infrared laser directly into a broad spectral range of good beam quality spanning from visible to infrared wavelengths. More strikingly, I have also unveiled and characterized experimentally an intriguing phenomenon of light self-organization in MMF, now known as Kerr-induced spatial beam self-cleaning. This effect allows for significant increase of spatial beam quality and brightness enhancement, and is remarkably immune to external perturbations like stress or bending. Indeed, this unexpected discovery demonstrates that Kerr effect has the capacity to form a highly stable, spatially bell-shaped beam close to the fundamental fiber mode, when starting from the typical irregular speckled pattern obtained in the linear regime at multimode fiber output (*K. Krupa et al., Nat. Phot. 11, 237, 2017, 343 citations without self-citations from Scopus*).

These results permit to shed new light and more profound understanding on spatiotemporal dynamics of multimode beams by stimulating numerous scientific discussions and further research works. Interestingly, the physical mechanism behind such a peculiar beam self-cleaning phenomenon is still unclear, and its intriguing connection with classical wave condensation and thermalization theory remains under constant debate *(M. Ferraro et al. Advances in Physics: X 8, 1-35, 2023)*. My achievements have attracted much interest by

several research groups over the world, willing to reproduce and study those two effects also in other experimental settings (*Z. Eslami et al., Nat. Comm. 13, 2126, 2022; H. Poubeyram et al., Nature Physics 18, 685-690, 2022*). Moreover, besides their relevance as a test-bed for fundamental research, these findings have very promising applications in development of novel photonic devices such as spatiotemporal mode-locked fiber lasers and amplifiers and novel broadband light sources (*L. G. Wright et al., Science 358, 94, 2017; U. Teğin et al., Optica 6, 1412, 2019*) for spectroscopy and biomedical nonlinear imaging. I have contributed to implementation of some of those applications in the framework of collaboration. They will be briefly discussed at the end of this research paper cycle.

My findings, related to the study on multimode fibers, have resulted in total in more than 40 articles in top-ranked journals and more than 80 conferences including more than 30 by invitation (e.g. I gave several invited talks at renown international conferences and one tutorial talk at the CLEO Pacific Rim conference 2022), 2 book chapters, as well as 3 international patents. Moreover, my research has triggered strong interest of an international audience being presented in several review papers (*L. G. Wright et al., Nat. Phys. 18, 1018, 2022; J. Bloch et al., Nat. Rev. Physics 4, 470, 2022; L. G. Wright et al., Optica 9, 824, 2022*) and the chapter 14 of G. P. Agrawal book "Nonlinear Fiber Optics" 6th Edition.

Among all the related articles of my co-authorship, I selected 13 of those papers discussing my major contribution to the research on multimode fiber optics while also reflecting the entire cross-section of my work in the field [**1-KK,…,12-KK**]. Below, I provide detailed description of their content starting with the introduction of the research context, state of the art and motivations behind this work. A broad overview of the recent research on multimode dynamics including my strong contribution is presented in my review article [**11-KK**]. My other achievements beyond the subject of this research paper cycle are briefly presented in the section 5, instead.

Introduction: Motivation and State-of-the-art

Multimode optical fibers (MMFs) have been investigated for several decades, starting from the 1970s. Early work considered their capacity to transmit information over multiple spatial channels. Many studies have also been devoted to exploring the consequences of the linear and nonlinear coupling among multiple guided modes and their different velocities including interactions among several lasing modes. This involves early investigations of the nonlinear phenomena in MMFs such as, for instance, self-focusing effect, self-phase modulation (SPM), four-wave-mixing (FWM) and stimulated Raman scattering (SRS), to name a few [1-4]. The concepts of multimode soliton and multimode mode-locking were also formulated and theoretically analyzed at that time [5,6].

When light propagates in MMFs, it experiences an inherent randomization, which is typically attributed to the linear mode coupling caused by mechanical perturbations and technological deviations from the ideal fiber structure, allowing excitation of a large number of guided modes. As a consequence, it is usually considered that MMFs deliver spatially low-quality light affected by speckle distortions. Large modal dispersion of MMFs additionally spoils information encoded in time domain, severely limiting the use of MMFs in many applications. Moreover, the beam propagation carried by a multitude of transverse and longitudinal modes is a highly complex spatiotemporal process. It requires advanced numerical tools to be simulated, which were hardly or even not available in the past. That is why the interest in MMFs rapidly started to wane by the early 1980s with the advent of single-mode fibers (SMFs) in what concerns both scientific research and industrial applications, leaving nonlinear properties of MMFs greatly unexplored. Indeed, supporting only one fundamental mode, SMFs in addition

to their structural simplicity, provide high bandwidth and high spatial quality of delivered light. They can be described by purely temporal dynamics by applying way simpler, one-dimensional (1D) models.

The modern world of several important technologies has been then constructed around standard SMFs. However, SMFs have an inherent major drawback, namely their small mode area and low damage threshold that reduce the output energy available. For this reason, supercontinuum (SC), fiber amplifiers and fiber laser sources based on SMFs are of limited use for extremely high-energy applications. When using large mode area (LMA) fiber designs, the beam quality can be high, however it tends to be unstable as it depends on the relative phase between the fundamental and the higher-order modes (HOMs). Moreover, under certain operating conditions, the LMA fiber lasers are subject to transverse mode instabilities, which spoils their output spatial coherence [7]. In current telecommunication systems, instead, the used SMFs limit the capacity of available data rate, which is expected to be attain in very near future.

In this context, the interest of MMFs returned after 2005, being partly motivated by space-division-multiplexing (SDM) in optical communication systems. MMFs have been considered as a promising solution to the foreseen capacity crunch problem, since in contrast to SMFs, they can support a multitude of transverse eigenmodes, each with different spatial shapes and propagation constants. Since 2010, we have observed a strong resurgent of interest in the investigations of the nonlinear dynamics of multimode light interactions in optical fibers, with an exponential growth of number of articles published and cited each year (see Web of Science).

MMFs add a new dimension in optical wave propagation, which offers a world of new physics and new potential applications compared to those supported by single-mode devices that extends far beyond communications. Exploiting multimode and spatiotemporal nonlinear processes has been expected to bring novel opportunities and perspectives in the development of high-power laser sources and high-resolution imaging and sensing. Novel and exotic solutions in generating new wavelengths, new spatial shapes and in scaling the peak power might become possible.

Although significant progress is being made over the last years in understanding and controlling multimode waves, for the most part, these applications still require major developments before they become practical. This is because of the complexity of multimode fiber optics that presents major challenges. On the other hand, recent theoretical and computational advances can be extremely helpful in understanding, controlling and then exploiting new potential experimental discoveries in MMFs. In this regard, relatively efficient techniques for simulating the propagation of intense pulses in multimode waveguides have been developed [8], including notably the generalized multimode nonlinear Schrödinger equations (GMMNLSE) that has allowed to understand the observed behaviors. When many modes are excited, all of them can be coupled in principle, making the physics conceptually difficult, although extremely interesting from the point of view of fundamental science.

Indeed, MMFs provide an excellent and natural testbed for studying collective dynamics based on complex interconnections among a large number of basic elements, where nonlinearity, dissipation, and disorder can be, in principle, controllably included. They host a rich landscape of novel spatiotemporal phenomena to be discovered that could not be predictable on the basis of the propagation of the individual modes. Among the first recent discoveries we should mention, for instance, the concept of multimode temporal soliton, that is a short pulse that propagates with a single group velocity, resulting from nonlinear mode coupling that compensates for modal dispersion. As discussed above, the multimode temporal solitons were predicted long ago, but only recently were experimentally observed by the group of F. Wise [9]. The dispersive waves generated by these self-sustained nonlinear waveforms were soon after

experimentally revealed [10], as well, with a possibility of shaping the SC in the anomalous pumping regime thanks to its spatiotemporal nature [11]. The interactions among the multimode solitons have been studied numerically by the group of G. P. Agrawal, instead [12]. These are the examples of a few first papers published since the re-emergence of the field of multimode waves. However, since then there have been many different research groups involved in this research area, ranging from groups with focus on fundamental physics to groups with focus on applied research. The exhaustive overview of research performed over the last more than ten years is presented in [**11-KK**] including my contribution to the field.

Summary of my research results

Kerr-induced beam self-cleaning

The physics of complex systems has been inspired by the observation that a multitude of interacting elements can give rise to collective effects whose nature cannot be explained when these elements are taken singularly. Phase transitions from liquid to solid, for example, are evident at the macroscopic level of an ensemble of interacting molecules, and they cannot be fully understood through the microscopic picture of molecules taken singularly. In optics, the light complexity has recently attracted a strong research attention. The light-waves can propagate either in a bulk or in waveguide dielectric media with a plurality of modes, whose interactions can be mediated by the nonlinear response of the dielectric medium.

In this context, MMFs represent an ideal platform to study nonlinear light complexity since the interactions among their guided modes, via the Kerr nonlinearity of silica glass, is particularly efficient, owing to the relatively small field confinement. As mentioned above, MMFs have usually been considered as unreliable optical systems because of the common belief that the light experiences an inherent randomization in these multimode waveguides, whenever propagation involves a relatively large number of guided modes. As a matter of fact, an input laser beam of high spatial quality leads to an irregular speckled structure resulting from mode interference when emerging at the output of MMFs. Moreover, typical fiber perturbations such as stress, bending, or temperature variations lead to sudden variations of this speckled pattern.

However, in my first breakthrough experiment discussed in [**3-KK**] I have demonstrated that, unexpectedly, at sufficiently high input power, when increasing the length of a graded-index (GRIN) MMF to above a few meters, or when looking at the fiber output when increasing the input power above a certain threshold value, the transverse profile of the beam self-cleans, strongly reducing the modal noise. In other words, the light beam emerging from the GRIN MMF reshapes into a bell-shaped profile in the center, resembling to the fundamental mode of the fiber, sitting on a low power multimode background. It is interesting to note that this effect vanishes by bringing down the input power below the threshold value, and can be restored as the input power is increased again. Note that this novel phenomenon enables self-organization of spatiotemporal content of multimode light beams by exploiting nonlinearities instead of relying on complex devices for input/output mode composition control [13]. It has the peculiar property of significantly increasing the beam brightness at the output of a MMF. This situation is in striking contrast to the known phenomenon of the beam clean-up obtained via SRS or stimulated Brillouin scattering (SBS), whereby the down-converted Stokes waves are preferentially generated in the fundamental mode of the fiber [3,14]. Here, the beam cleaning manifests at the pump wavelength itself, thanks to the intensity-dependent refractive-index change (see section *Physics of beam self-cleaning phenomenon*), thus in the literature it has been named the Kerr-induced beam self-cleaning. It proves that the light itself has the capacity

to trigger a self-organization process. The beam self-cleaning has been observed before reaching the threshold for SRS and any spectral broadening or frequency conversion occurs. This effect is then completely different from the catastrophic self-focusing, which requires peak power orders of magnitude larger than the one leading to the Kerr self-organization in a cleaned beam. It is also important to point out the fact that the phenomenon of Kerr self-cleaning is remarkably robust against the presence of relatively strong external mechanical perturbations such as squeezing and bending of the fiber, a situation markedly different from what happens in the multimode linear regime. This feature is particularly essential from application point of view as will be discussed later in this report.

In what follows, I will describe the manifestations of Kerr beam self-cleaning in various optical fiber systems including conservative [**3-KK, 10-KK**] and dissipative settings [**4-KK**]. The complete characterization of such process, including its temporal [**6-KK**], spectral [**3-KK**] and polarization [**8-KK**] dynamics will be reported followed by the possible applications [15-17]. Finally, I will discuss the hypothesis concerning physical mechanisms responsible for the Kerr beam self-cleaning [**9-KK,** 18,19].

Experiment in fiber conservative system

As mentioned above, I have first discovered and studied experimentally the effect of Kerr-induced beam self-cleaning in lossless propagation environment, in particular in standard commercially available GRIN MMFs in the normal dispersion regime with sub-nanosecond pulses [**3-KK**]. In this first experiment, 900 ps pulses with 30 kHz repetition rate delivered by an amplified Nd:YAG microchip laser operating at 1064 nm were lunched into 12m-long GRIN MMF with 52 μm of core diameter. Using a Gaussian beam of about 40 μm in diameter, tens of guided modes were simultaneously excited.

Figure 1 shows the self-cleaning effect manifesting as a spatial beam reshaping. Indeed, panels (a)-(d) of Fig.1 present the near-field beam patterns emerging at the fiber output at 1064 nm as a function of the output peak power (P_{pp}). Whereas, panels (a')-(d') of Fig.1 illustrate the corresponding beam transverse profiles. As we can see, at relatively low powers (P_{pp} = 3.7 W), that is in linear regime, the input Gaussian beam takes a form of a random speckles as a result of highly multimode excitation (see Figs.1(a) and (a')). However, unexpectedly when increasing the input pulse power, the output beam profile has progressively evolved from highly irregular to a well-defined spot in the core center, whose diameter is close to the fundamental mode of the fiber, surrounded by a residual low-power speckled background (see Figs.1(d) and (d')).

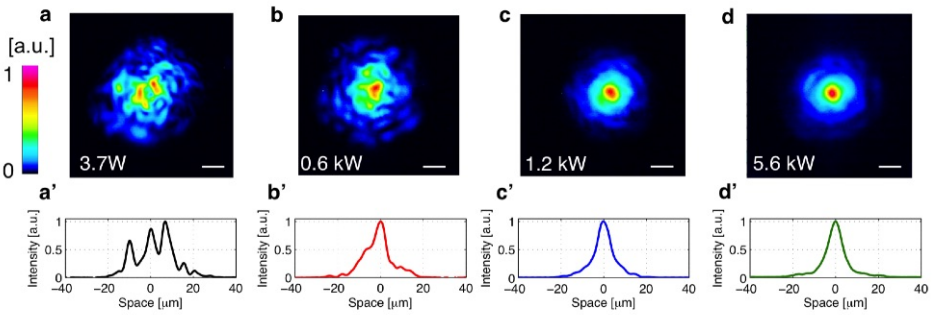

Fig.1 (a-d) Experimental evolution of near-field pattern of the GRIN MMF output at 1064nm as a function of output peak power P_{pp} (the color code refers to intensity levels normalized to the local maximum). Scale bar: 10μm; (a'-d') Corresponding beam profiles versus x (y=0). Fiber length: 12m. Reproduced from [**3-KK**].

The important feature of the beam self-cleaning effect is its ability to significantly improve the quality of the multimode output beam and its brightness. Indeed, as illustrated in Fig.2, I measured a nearly threefold decrease of the output near-field beam full width at half maximum intensity (FWHMI) diameter (red circles), further confirmed by measurement of the M^2 beam parameter (not shown here). The data points given by the blue squares in Fig.2 show instead the fraction of power at 1064 nm carried by the central part of the beam measured with a diaphragm opened at a diameter of 12 μm as a function of total output power at 1064 nm. We can clearly observe that the power in the center of the beam first increases nearly linearly up to the power threshold for beam self-cleaning, where an abrupt increment in slope by a factor 5.3 occurs. The linear behavior beyond the power threshold indicates the establishment of a new equilibrium in the energy distribution between HOMs and the fundamental mode.

Moreover, we experimentally verified that the redistribution of power towards a central bell-shaped profile results neither from additional transmission losses, nor from loss of spatial and temporal (frequency conversion) coherence. We carried out Young's double-slit experiment and as presented in Fig. 3 and we obtained interference fringes with a similar contrast of 70% when the two interfering parts of either the initial speckled beams (see Fig.3(a)) or of the self-cleaned beams (see Fig.3(b)) were spaced by a distance nearly equal to the beam diameter.

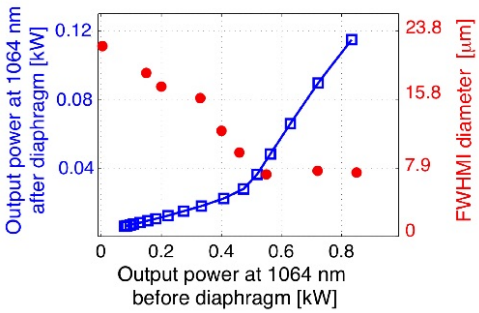

Fig.2 (blue open squares) Output power at 1064nm measured in the central part of the fiber as a function of the total output power; (red filled circles) Corresponding FWHMI diameters of the near-field beam at 1064nm. Reproduced from [**3-KK**].

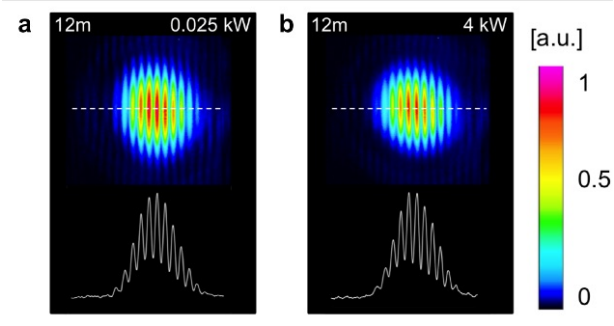

Fig.3 Examples of near-field interference patterns obtained in Young's double-slit experiment obtained in the linear regime (at P_{PP} = 0.025 kW) and (b) in the beam self-cleaning regime (at P_{PP} = 4 kW); Reproduced from [**3-KK**].

Then, we further analyzed the fine structure of the spectral evolution in the process of beam cleaning. The fiber output was imaged on a CCD camera through a special dispersion grating allowing to resolve the longitudinal modes of the microchip laser. With this setup, it was possible to obtain an image that combines the transverse spatial pattern (in vertical coordinate) and the frequency spectrum of very high resolution (in horizontal coordinate). The obtained results for increasing peak power are displayed in Fig.4. As we can see, at low powers (see Fig.4(a)) the output spectrum is characterized by a nearly single longitudinal mode of the input laser, with a weak second longitudinal mode, slightly down-shifted in wavelength (by about 200 pm). Whereas, in transverse dimension, as expected and mentioned above, the output beam exhibits an extended speckled spatial pattern, owing to the multimode propagation. However, when we increased the peak power, the light beam relocates its power towards fiber center, as clearly demonstrates the vertical axis (see Fig.4(b)). Importantly, while this occurs, the spectrum indeed remains essentially unchanged, keeping a constant size in the horizontal direction. For an even stronger peak power value, the transverse previously cleaned beam is preserved, but now the spectrum is broadened by SPM (see Fig.4(c)). Note that in this experiment a shorter, 3m long GRIN MMF was used, which explains the corresponding higher level of power that was required for observing self-cleaning. Indeed, the Kerr beam self-

cleaning depends on the product of fiber length times power. Thus, it can be obtained with different powers and fiber lengths, provided that their product remains unchanged, in analogy to the Kerr effect in single-mode fibers.

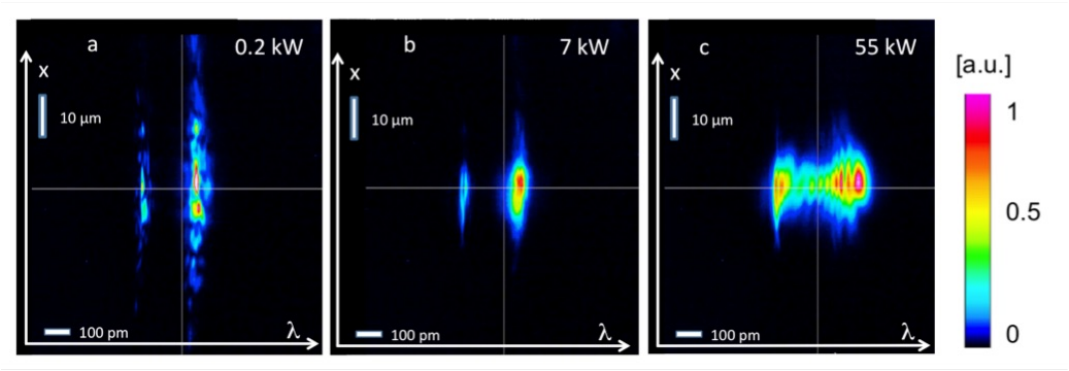

Fig.4 Spatio-spectral (x-λ) profile of the output beam at the output peak power (a) P_{PP} = 0.2 kW, (b) P_{PP} = 7 kW (beam self-cleaning regime) i (c) P_{PP} = 55 kW. Intensities normalized to local maximum. Fiber length: 3 m. Reproduced from [**3-KK**].

To study the dependence of the beam self-cleaning upon different input conditions, we studied also the variation of output beam diameter within a set of statistically significant number (1000) of different input conditions, and thus different speckle distributions at the fiber output. We varied the input conditions by changing the linear polarization of the input laser beam with a wave-plate and a micrometric angular displacement system, and we registered the output beam diameter at FWHMI, repeating the same procedure for different peak powers. The results are reported in Fig.5. At low powers, the significant variations in the speckled beam can be observed with large values of the standard deviations. This can be explained by the different speckle configurations induced by the variety of input conditions that could be excited: two markedly different examples are illustrated in the insets of Fig.5. Note however that, a strong reduction of these beam width fluctuations was observed at high powers (i.e., above 2 kW). In this regime, because of beam self-cleaning, the beam at FWHMI is only weakly influenced by any variations of the input conditions: at high powers, there is a dramatic reduction in the standard deviation, as well as a significant reduction of the average diameter.

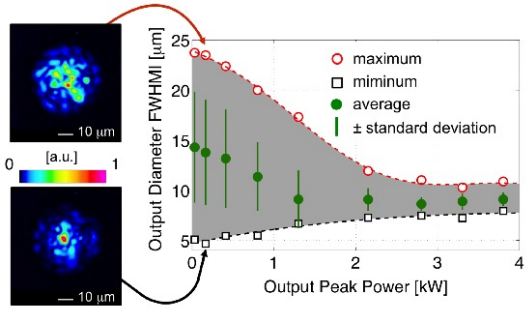

Fig.5 Values of the FWHMI diameter as a function of the output power calculated from 1000 different input conditions. Insets: examples of near-field images of two 'extreme' spatial beam distributions recorded at P_{PP} = 0.1 kW. Fibre length: 12 m. Reproduced from [**3-KK**].

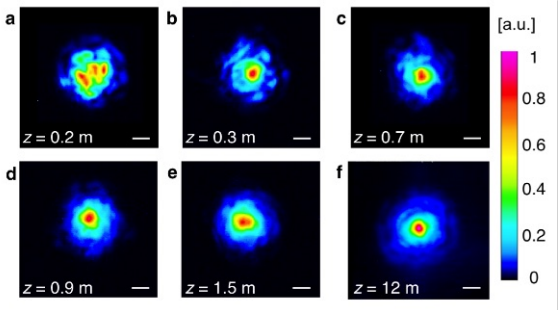

Fig.6 Experimental evolution of near-field pattern of the GRIN MMF output at 1064nm and at P_{PP} = 44 kW as a function of propagation distance *z* (Intensities normalized to local maximum). Scale bar: 10µm. Reproduced from [**3-KK**].

To gain further insight into the beam self-cleaning process, I also performed a cut-back measurements. Figure 6 shows the near-field beam profile taken at the fiber output at P_{pp} = 44 kW by gradually backward cutting the fiber. Despite the relatively high power used in these experiments, the input Gaussian beam still splits into several guided modes along the first few

hundreds of millimeters to produce spatial speckles (see Fig.6(a)). The observed scrambling of the initial phase front proves that, immediately after coupling light into the fiber, transverse beam evolution is predominantly affected by mode beating owing to their different wavenumbers. Progressing further along the fiber, the cut-back analysis confirms that strong spatial reshaping occurs along the propagation direction similar to what was observed at the fiber output with a power increase. This observation also proves that the onset of beam self-cleaning is activated in the presence of a multimode excitation.

It is also worth to mention, that our further experiments [20] demonstrated that it is also possible to self-clean towards modes, which are different than the fundamental mode of the fiber. Indeed, by varying the input launching conditions, thus the combination of excited guided modes and the nonlinear mode coupling among them, we could achieve beam cleaning at several low-order modes. By wavefront shaping of the input beam it was even possible to call on demand the desired low-order mode.

Experiment in fiber dissipative system

The experiments described in the previous section demonstrate beam self-cleaning in lossless environment of GRIN MMFs (i.e. when absorption is negligible). Now, one can wonder whether the same phenomenon can be also observed in dissipative system of MMFs doped with rare earth atoms, especially since active fibers available on the market have step-index profile rather than of parabolic shape.

The experimental results presented in [**4-KK**] demonstrate that again, quite surprisingly, the beam self-cleaning can also occur, whenever the linear propagation is strongly dissipative. We analyzed two different configurations: the first further called passive or lossy configuration where beam propagation took place in the presence of strong distributed losses without any pumping. In the second configuration, the doped fiber was pumped by a CW laser diode, and this configuration will be called the active one, owing to the presence of optical gain. In those experiments, we used a 3 m long double-clad Ytterbium-doped MMF fiber (Yb-MMF) with a core of 50 μm in diameter surrounded by a D-shaped inner cladding (340μm x 400μm in size). This fiber had a non-parabolic refractive index profile, which was mostly step-index with a weak residual quasi-gradient shape in the core center. The Ytterbium doping distribution was measured to be quite uniform in the core. As a signal beam, we used a microchip Nd:YAG laser delivering a 1064 nm Gaussian beam of 500 ps pulses at 500 Hz.

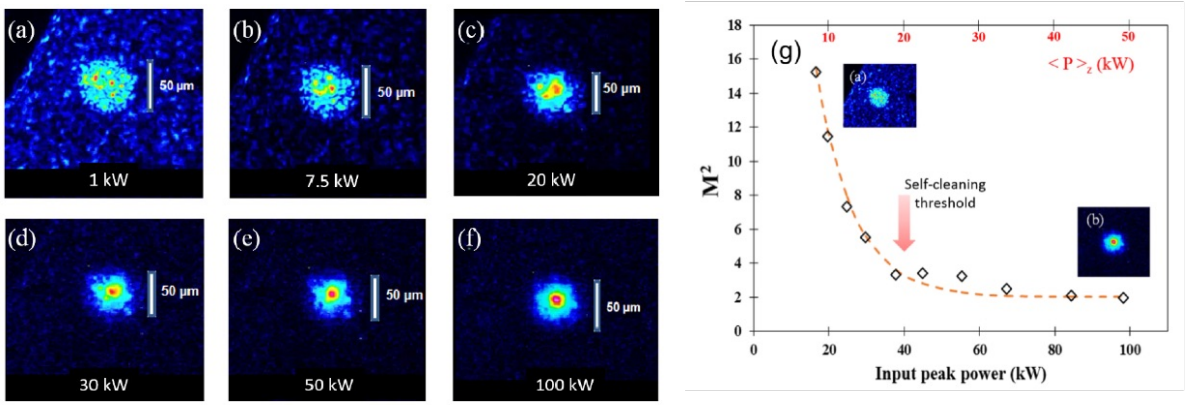

Fig.7 (a-f) Near-field patterns recorded at the output of the passive double clad Yb-doped MMF for various levels of the input peak power (P_{in}). The pump laser was switched off. (g) Corresponding M^2 measurement as a function of P_{in}. Reproduced from [**4-KK**].

In the experiment in a passive configuration (without a gain) the 1064 nm signal beam was focused at the input face of the Yb-MMF with a spot size of nearly 22 μm at FWHMI allowing for multimode excitation. The near-field beam evolution as a function of input power is illustrated in Fig.7. Interestingly, despite the large overall attenuation of about 7.3 dB (2.44 dB/m at 1064nm) and the non-parabolic refractive index profile, it was still possible to observe beam cleaning effect. In particular, when increasing the input beam power, the output pattern, which was highly speckled at low powers (see Fig.7(a)) evolved into a smooth bell-shaped spot, surrounded by a residual low-power, multimode background (see Fig.7(f)). The M^2 parameter of the output beam dropped from 16, in the low-power regime, down to a value of only 2 after beam cleaning was reached, as illustrated in Fig.7(g).

However, it is worth noting that in this lossy case the nonlinear beam reshaping process was qualitatively different from the one previously described in the case of a virtually lossless GRIN MMF. With the Yb-MMF the input power was not only coupled into the multitude of the guided modes of the core, but also into the HOMs leaking into the D-shaped cladding. Note also that in the nonlinear regime, the doped fiber was less leaky than in the linear regime; the observed spatial beam reshaping into the quasi-fundamental mode was accompanied by an increase by a factor of 1.8 of the fractional output power carried by the fiber core and a significant reduction of the degree of coupling into the leaky HOMs. The total power transmission (MMF core + cladding) of the fiber was verified to be constant when the input power was varied.

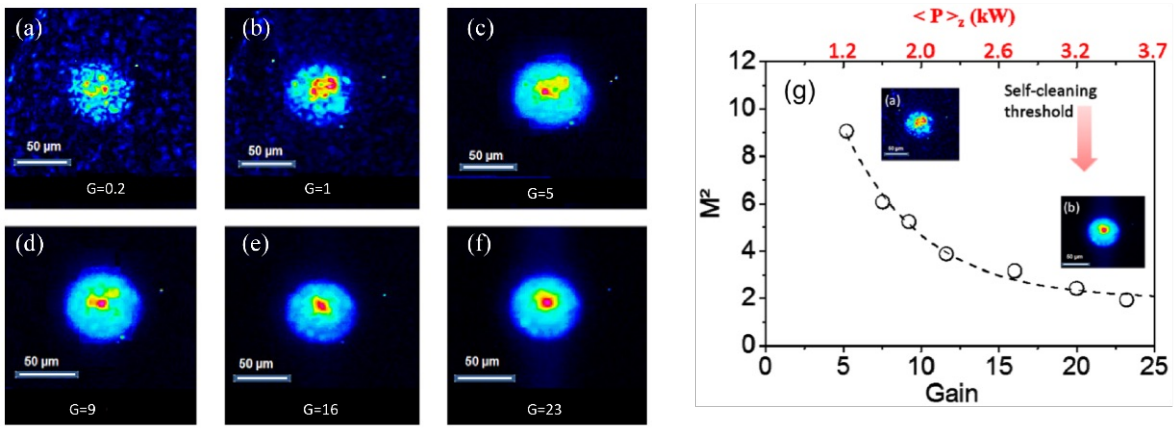

Fig.8 (a-f) Near-field patterns recorded at the output of the active double clad Yb-doped MMF for various gain levels (G) and for an input peak power of 500W. The pump laser was switched on. (g) Corresponding M^2 measurement as a function of G. Reproduced from [**4-KK**].

Next, we investigated the role played by a gain in the beam self-cleaning process, as more interesting case for potential application to development of multimode fiber lasers and amplifiers. We fixed the 1064 nm signal at the relatively low power level of 0.5 kW, and we pumped the D-shaped inner cladding of the Yb-MMF with a CW laser diode at 940 nm. A 3 nm wide spectral filter at 1064 nm was used at the fiber output to block the residual pump radiation, to remove most of the amplified spontaneous emission, and to filter out the amplified signal light. Figure 8 illustrates the evolution of the output near-field pattern upon the optical gain (G), which grows when increasing the pump power. The gain corresponds to the ratio between the measured output average power and the measured coupled power at 1064 nm. Again, the observed spatial modification is very similar to what was obtained in the passive (unpumped) configuration, and it is also similar to the Kerr beam self-cleaning effect observed in a conservative fiber system of GRIN MMF. The corresponding decrease of the M^2 parameter, from 9 down to 2, as presented shown in Fig.8(g), further confirms the substantial improvement of the output beam quality thanks to the self-cleaning effect. Such a result was reached for a gain G = 20, and with a signal input peak power of only 0.5 kW. Whereas, an input peak power

as high as 40 kW was required when the Yb-MMF was not pumped, that is around five times bigger than in the lossless case of a GRIN MMF of similar core diameter and length. However, importantly when comparing the power threshold expressed in terms of path-averaged power ($<P>_z$) its value significantly decreases (by about six times) by the presence of gain with respect to the case with loss. The presence of gain can then substantially facilitate the Kerr beam self-cleaning.

Moreover, it is interesting to notice that if we consider the power threshold of self-cleaning as expressed in terms of the output peak power instead, both values obtained in the Yb-MMF with and without gain remain close to the one measured in the lossless GRIN MMF for the similar fiber length [21]. This is presented in Fig.9, which provides a comparison of the longitudinal power evolution in the passive (without gain) and in the active (with gain) Yb-MMF. Note that in both experiments in dissipative configuration, we did not observe any spectral broadening accompanying the spatial beam reshaping.

These experiments clearly demonstrate that the beam self-cleaning exhibits a robust wave dynamics that is of a more general nature than what was initially thought. In fact, we found that the nonlinear spatial reshaping is not limited to strictly conservative systems, and to the fibers with purely parabolic index profile.

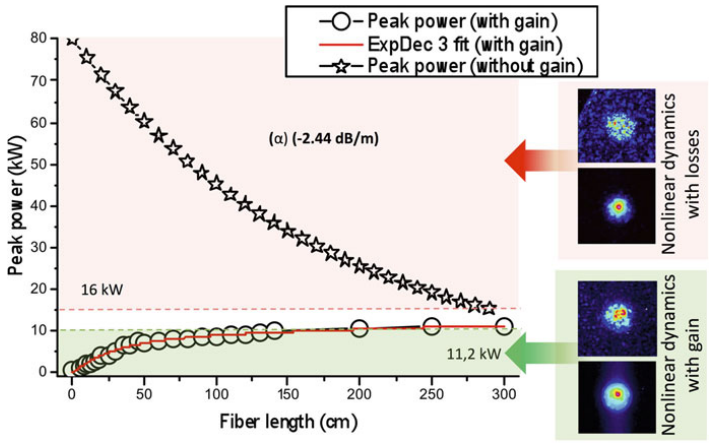

Fig.9 Comparison of the power evolution along the lossy and the active Yb-doped MMF, leading to self-cleaning in both cases. Reproduced from [21].

Temporal dynamics of conservative Kerr beam self-cleaning

Since the Kerr beam self-cleaning is an inherently spatiotemporal nonlinear process this section will address its temporal dynamics. My experiment revealed that, as it was discussed in [**6-KK**], the Kerr beam self-cleaning is accompanied by significant temporal-reshaping, that can be explained in the theoretical framework of the pulse self-switching in nonlinear coupled mode device. Moreover, for input powers slightly larger than the threshold value for Kerr beam self-cleaning, the sub-nanosecond laser pulses undergo up to four-fold shortening, associated with peak power enhancement.

Here, the same 12-m-long standard GRIN 52/125 MMF was used and pumped by the amplified microchip Q-switched laser delivering linearly polarized 1064nm pulses of 740 ps at a repetition rate of 27 kHz. The injection conditions were also similar to those applied previously. To measure the temporal profile of the output pulse train, I used a fast photodiode connected to a 20-GHz bandwidth real-time oscilloscope that was triggered by a small fraction of the same

laser. The output beam was magnified to let the photodiode detect only its central part corresponding to the fundamental fiber mode. The detected beam was also spectrally filtered with a 3-nm bandpass filter at 1064 nm.

Figure 10 illustrates a collection of output temporal waveforms that were measured for different input peak powers. It can be seen that the nonlinear temporal reshaping of the output pulse occurs for input power levels above 0.3 kW, which is well below 1kW, the threshold for beam self-cleaning. This indicates that nonlinear mode coupling starts before the observation of the spatial beam reshaping. Note that the influence of chromatic and modal dispersion effects on pulse propagation is negligible, owing to the long pulse duration and the short length of the fiber. By further increasing the input power up to 0.8 kW, a single nearly two-fold shorter peak forms at the center of the output pulses sitting on low power wings. When the input power grows larger the temporal reshaping continues with a recurring behavior, that is composed by a series of temporal broadenings, followed by the formation of a dip at the pulse center and then the growth of a narrower peak. At 4.5 kW, the output pulse duration compresses down to only 175 ps, which is more than fourfold shorter than the input pulse duration, resulting in around two times increase of the output peak power, since half of the energy is estimated to remain in the low power pulse wings. For input peak above 5 kW, an efficient Raman conversion occurs which leads to a power-dependent energy depletion of the output pulses measured at 1064 nm. Note that despite the transfer into the Stokes wave of a part of the beam energy, the spatial-beam cleaning remains active.

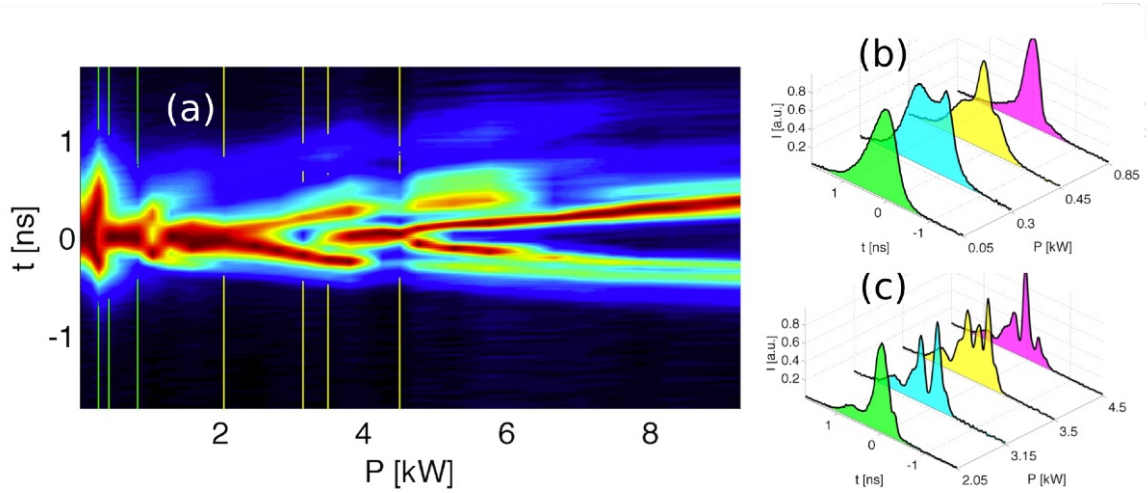

Fig.10 (a) Output temporal waveforms upon input peak power. (b,c) Corresponding waveforms at peak powers indicated by the vertical lines. Reproduced from [**6-KK**].

Such recurrent spatiotemporal nonlinear dynamics can be understood in the theoretical framework of the mode self-switching in nonlinear coupled mode devices; here, between the sampled fundamental mode and other HOMs. As previously mentioned, the photodiode placed at the center of the output beam essentially samples the fraction of the fundamental mode emerging from the multimode fiber. Now, different portions of the long pulse self-switch independently of each other, as it would be at different instantaneous power values. When the instantaneous power reaches the value large enough to switch to fundamental mode, the output power in the center of the beam is enhanced. The low-power pulse wings remain largely undistorted. This tendency is enhanced, when the self-cleaning increases the fundamental mode content. This explains the reduction of the observed pulse temporal duration. As the peak power grows larger, the wings of the pulse have now a sufficient power to experience self-cleaning into the fundamental mode, whereas the power at the pulse center is so high that the output

spatial mode switches to another low-order mode with a spatial distribution with a dip at the center; the photodiode would detect this situation as a reduction of instantaneous power, thus temporal profiles with a hole in the center are observed. The described phenomenology is universal to nonlinear coupled mode devices: for example, very similar nonlinear pulse reshaping occurs in the self-switching of a two-mode nonlinear birefringent fiber [22].

The presented above hypothesis about the nonlinear mode self-switching or nonlinear mode coupling was further confirmed by implementing a novel time-resolved mapping allowing to measure spatial pattern at each instant of time with picosecond temporal resolution [23]. Indeed, with such a real-time spatiotemporal technique, we provided the first unambiguous experimental evidence of spatiotemporal instantaneous nonlinear periodic power exchange among the modes of the GRIN MMF, particularly between its fundamental and HOMs. We characterized in real time nonlinear mode coupling leading to Kerr beam self-cleaning across the pulse duration. Consequently, with this method we also reproduced and thus confirmed the recurrent behavior of temporal reshaping discussed above.

Polarization dynamics of conservative Kerr beam self-cleaning

This section will be devoted to the polarization dynamics of Kerr beam self-cleaning that I studied with a series of ad hoc experiments, and which were discussed in [**8-KK**].

I used again a 11-m-mong fiber of type 52/125 GRIN MMFs commercially available. The fiber was pumped by a Nd:YAG microchip laser delivering 500 ps pulses at 1064 nm and a repetition rate of 500Hz in a way to obtain multimode excitation. The input beam had a Gaussian spatial shape and a linear state of polarization (SOP). To analyze the SOP of the output beam in the process of beam self-cleaning, I measured the averaged in time and space Stokes parameters of light, S_0, S_1, S_2, S_3, following the classical method originally proposed originally by Stokes in 1852. Then, I calculated the total degree of polarization $DOP = \sqrt{S_1^2 + S_2^2 + S_3^2}/S_0$, the degree of linear polarization $DOLP = \sqrt{S_1^2 + S_2^2}/S_0$, the degree of circular polarization $DOCP = S_3/S_0$, and the azimuth of linear polarization $\tan(2\psi) = S_2/S_1$ [24].

It is known that in non-polarization-maintaining optical fibers, the polarization components of guided modes are linearly coupled, owing to the unavoidable presence of weak random birefringence, which is induced by manufacturing imperfections, and by externally applied stress or bending. Consequently, in linear propagation regime, a linearly polarized laser beam gradually loses its DOLP when it propagates along a MMF.

My work presented in Fig.11(a) (blue dots) shows that when the input peak power grows larger and the beam propagation enters to nonlinear regime, the DOLP measured at the output of the GRIN MMF first rapidly increases from 0.1 up to 0.26 when the input power crosses the power threshold for Kerr self-cleaning (~3 kW) reaching maximum at P_{in} = 4 kW, and then decreases when the beam power grows larger. It is reasonable to think that since the size of the fundamental mode, here around 7.45 μm at FWHMI, is much smaller than the core diameter of the GRIN MMF, which is of 52 μm, the SOP of the light carried by the fundamental mode is relatively insensitive to technological irregularities and external disturbances along the fiber. The Kerr beam self-cleaning partially transfers the power towards the fundamental mode being a robust effect preventing further energy leakage out of the fiber center. Such nonlinear dynamics may thus explain the observed initial repolarization, and the associated ~2.5-fold increase of DOLP. The subsequent decrease of DOLP for higher powers may result instead from the effect of nonlinear polarization rotation, combined with temporal averaging across the

pulse profile: different time sections rotate their output SOP by different amounts decreasing the DOLP taken in average. Indeed, as presented in panel (b) of Fig.11, a shift of the azimuth ψ of the main linear polarization axis starts to increase above P_{in} = 4 kW. Note that the nonlinear polarization rotation in MMFs has been later used to implement an ultrafast saturable absorber mechanism for multimode fiber lasers [25]. To complete the characterization of the output light SOP, in panel (a) of Fig.11, we also present the measurements of the output DOCP and DOP versus input power are also reported by green triangles and red squares, respectively.

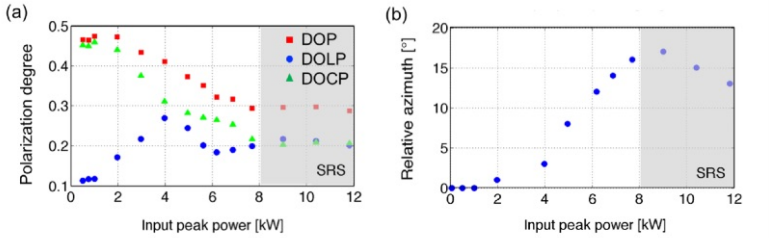

Fig.11 (a) Measured DOLP (blue dots), DOP (red squares), and DOCP (green triangles) as a function of input peak power (P_{in}); (b) Relative azimuth of linear polarization as a function of P_{in}. Gray area - regime of SRS generation. Reproduced from [**8-KK**].

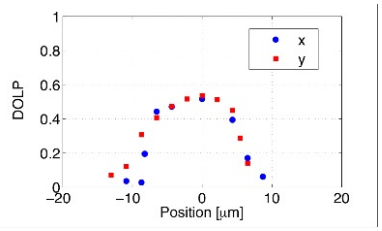

Fig.12 DOLP as a function of transverse position across the beam along x-axis (y=0) (blue dots) and y-axis (x=0) (red squares), at P_{in}=4 kW. Reproduced from [**8-KK**].

Next, I analyzed the spatial distribution of the output DOLP in the regime of the self-cleaning, by filtering the magnified output near-field with a movable diaphragm. The results are presented in Fig.11, in which blue and red dots represent the results measured along the horizontal and vertical cross section of the output beam. As can be seen, at the beam center, the DOLP has the largest value up to 0.6, which again confirms that the self-cleaning leads to the partial nonlinear re-polarization of the light propagating in MMFs.

Finally, I investigated the influence of the beam diameter at the input of the fiber on the polarization dynamics in the regime of Kerr beam self-cleaning. The obtained results of DOLP measurements at the fiber output are shown in Fig.12, with the corresponding near-field images in the insets. DOLP decreases when the spot diameter grows larger. Focusing the beam at the fiber input face with a larger diameter allows excitation of larger number of modes, so that the excited fundamental mode has lower energy. Consequently, the self-cleaning-induced energy transfer towards the fundamental mode, and the associated nonlinear re-polarization, are both less efficient, resulting in smaller increase of DOLP.

Physics of beam self-cleaning phenomenon

The light self-organization effect of beam self-cleaning, that I observed for the first time in 2017 in silica GRIN MMFs pumped with sub-nanosecond beam at 1064nm, has been subsequently experimentally reproduced by other different groups in the world with laser pulses ranging from nanoseconds down to femtoseconds, and at wavelengths spanning across the entire transparency window of silica fibers, from the visible to the infrared region, as well as in fibers made of soft-glass materials [26-28]. However, strikingly, although several years have already passed the physical mechanism behind this peculiar effect is still the subject of a hot debate, remaining highly controversial in the research community.

A trivial explanation for the beam self-cleaning as a result of relatively higher nonlinear losses for HOMs was ruled out by my early experiment [**3-KK**] showing that the input/output power transmission remains strictly linear at all intensities involved. Another possible mechanism via

the loss of spatial coherence resulting from nonlinear spectral broadening was also quickly disproved in the same experiment [**3-KK**] (see section *Experiment in fiber conservative system*). Indeed, at the onset of beam cleaning the SPM induced broadening remains negligible, in particular for sub-ns pulses, while self-cleaned beams maintain the spatial coherence of the source, as demonstrated by double slits experiments [**3-KK,** 29].

As a matter of fact, we developed a first tentative explanation for the beam self-cleaning phenomenon and its nonlinear asymmetry of power flow toward the fundamental mode of the GRIN MMF, basing on the nonlinear non-reciprocity of the mode-coupling process developed in the framework of a simplified two-mode mean-field theory (MFT) [**3-KK**, supplementary Information].

In GRIN MMFs the propagation constants of the mode groups are equally spaced, letting the multimode beam experience natural oscillations when propagating in otherwise longitudinally uniform medium, called self-imaging effect. Such a periodic intensity focusing modulates longitudinally the fiber refractive index due to the action of Kerr effect leading to formation of a dynamic long-period fiber grating [30]. Such a grating may in turn provide quasi-phase-matching for a variety of nonlinear FWM processes, leading to energy exchange between the fundamental and the HOMs. The dynamics of such interactions between the fundamental mode and the HOMs in terms of an effective coupling term driven by the collective presence of all the fiber modes through FWM has been described by our MFT model in [**3-KK**, Supplementary Information]. Indeed, a key outcome of this model is the nonlinear non-reciprocal behavior of the equivalent nonlinear two-mode coupler. It predicts that, for powers above a certain threshold power value, the reciprocity of mode coupling is broken because of the presence of SPM, which is highly different for the fundamental and for the HOMs owing to the difference between their overlap integrals. Then, if the mode power distribution is initially in favor of the fundamental mode, the beam power remains in the fundamental mode. One can further speculate that, when extended to describe the collective interactions in the original complex multimode system, the nonlinear non-reciprocity model may smoothen the dependence on the initial conditions leading to irreversibility of the energy flow into the fundamental mode. The group of Prof. Stefan Wabnitz has demonstrated instead that the flow of energy towards the fundamental mode is accompanied by a flow of energy into HOMs, manifesting as a simultaneous occurrence of an inverse and direct energy cascade with an average mode number conservation [31].

Soon after its first experimental demonstration, a link between the Kerr beam self-cleaning with the theoretically predicted several years before classical multimode wave condensation [32] has rapidly attracted a strong research attention thanks to the remarkable resemblance of the signature of those two phenomena. The beam self-cleaning has been observed as a beam transformation occurring in GRIN MMFs from speckles into a bell-shaped beam sitting on a low intensity multimode background [**3-KK**]. Whereas, the wave condensation manifests by the spontaneous formation of a largescale coherent structure (fundamental mode) that remains immersed in a sea of small-scale fluctuations (background of HOMs with power equipartition) [32]. Moreover, the irreversible process of classical wave condensation has been predicted for purely conservative and formally reversible (Hamiltonian) systems of random waves under weakly nonlinear regime. It finds its origin in the natural thermalization of the wave system toward the thermodynamic Rayleigh-Jeans (RJ) equilibrium distribution. We may describe this thermodynamic state in terms of two macroscopic parameters, i.e., its temperature (T) and chemical potential (μ), which at equilibrium are uniquely determined by the energy (E) (it is called Energy because it is the linear contribution to the Hamiltonian, and it is a measure of coherence of the input beam) and by the number of particles (N) (i.e. the beam power, interpreted as total number of particles), which are fixed by the initial conditions. In fact, at a critical value of the energy (E_{crit}) (or the temperature (T_{crit})) the denominator of the RJ

distribution vanishes and this singularity (divergence to infinity) is regularized by the macroscopic population of the fundamental mode of the system. Note that in this particle-equivalent model, the fiber admits a finite number of guided modes and the power carried by a given mode is called the mode population. However, achieving complete thermalization and condensation of incoherent waves through nonlinear optical propagation at that time was known to require a prohibitive-large interaction lengths, far from being achievable in practical experiments.

Motivated by the discovery of the Kerr beam self-cleaning, Dr. Antonio Picozzi and Prof. Josselin Garnier have developed a new theory that has revealed how a weak disorder can significantly accelerate the process of thermalization and condensation even by several orders of magnitudes. Indeed, light propagation in MMFs is known to be affected by a structural disorder of the material due to inherent technological imperfections and external perturbations. Such striking finding has then allowed finally to interpret the effect of beam self-cleaning in the framework of classical wave condensation theory. Note that the discrete nature of the developed kinetic equation also explains why the beam self-cleaning has been only observed in parabolic-index optical fibers and not in step-index fibers, that is because the latter does not ensure the presence of effectively phase-matched FWM processes. Following this new theory, we performed a new experiment by properly shaping its initial conditions and demonstrated for the first time an effect of light condensation into the fundamental mode of the GRIN fiber [**9-KK**].

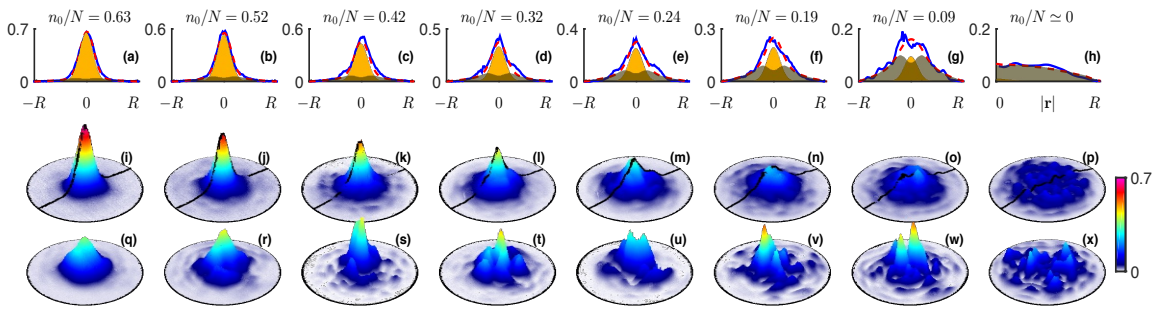

Fig.13 Experiments: Intensity pattern at Z_0=20 cm (i)-(p) and at the output of the fiber L=13 m (q)-(x). By reducing the number of initially excited modes (i.e., by decreasing E), a transition occurs from n_0=0 to a condensate fraction of $n_0/N \approx 0.63$. Reproduced from [**9-KK**].

The theory of classical wave condensation assumes an initial random power distribution among the excited modes. To assure those features and hence to adhere at the best to the requirements to prove experimentally this theory, we conceived a different system of light injection. Differently from what was done in the original experiment of beam self-cleaning, we injected the laser beam to the fiber through an optical diffuser, thus in a way to not privilege the excitation of any guided modes. Then, we fixed the power (N) and we varied the energy (E) (i.e. the coherence) by shifting the diffuser plate in its transverse plane; E increased (i.e. coherence decreased) as the beam populates the HOMs. With this experiment that was performed in 13m long GRIN MMF, we demonstrated experimentally the transition from spatially incoherent mode distribution to wave condensation, with a condensate fraction of up to around 60% in the fundamental mode of the waveguide as the coherence (E) of the input beam is increased. The results are presented in Fig.13 (the refractive index profile playing the role of trapping potential).

Then in another set of experiments, based on the measurements of the beam near- and far-field, we studied the mode power distribution at the output of GRIN fibers, and we experimentally

demonstrated that the beam self-cleaning is driven by optical thermalization toward the Rayleigh-Jeans (RJ) equilibrium [18].

It is important to mention that other research groups have also recently studied the mode power distribution at the output of GRIN fibers also showing that for the self-cleaned beams the probability of occupation of the fiber modes is closely reproduced by the RJ law [33,34]. Basing on those results the group of Prof. Demetri Christodoulides has described the wave phenomenon of beam self-cleaning in the framework of thermalization of the gas of particles (large number of guided modes), instead [35]. Currently, there are then two analogous yet different approaches resulting from thermodynamic theory: one based on the wave turbulence theory, and the second one derived in analogy to the gas of particles. The fundamental difference in experimental demonstration of both those approaches is the possible variation of the input power (N). While, the experiment demonstrating the former theory studies the beam output upon different input energies (E), at constant power (N), the experimental demonstration of the latter approach takes into consideration also cases where the energy (E) is fixed upon variation of power (N).

It is also important to underline that although the interpretation of the beam self-cleaning phenomenon in terms of a thermal equilibrium state of maximum entropy in the complex process of modal FWM is truly fascinating, it has its own strong limitations, since it allows to predict only the key properties of this effect [19]. Indeed, the Kerr beam self-cleaning is much more robust than one could anticipate from thermodynamic descriptions, which cannot capture some of its aspects discussed in previous sections of this report, such as, for instance, its capability to self-cleans also into other modes than the fundamental one, its capability to preserve the coherence of input beam, as well as its capability to occur under highly dissipative propagation conditions, e.g., in the presence of heavy loss or strong gain in active MMF. Note that a fixed propagation length of optical fiber does not necessarily ensure to be long enough to let the system reaching the thermal equilibrium distribution. Moreover, the wave condensation and thermodynamic pictures only account for the spatial properties of a multimode monochromatic continuous waves. Whereas, the beam self-cleaning also involves the temporal and spectral (see next sections) domains. As a matter of fact, some questions still remain open, leaving the ground for future work in this emerging field of research.

Geometric Parametric Instability

The self-organization arising from a complex collective dynamics of beam propagation in MMFs may also manifests in temporal domain as a spatiotemporal parametric instability (PI), with no equivalent counterpart in single-mode or few-mode fibers. First theoretically predicted by Stefano Longhi in 2003 [36], such type of peculiar instability was experimentally demonstrated by me for the first time only in 2016 as a generation of a multi-octave spanning series of unequally-spaced sidebands in graded-index (GRIN) multimode fiber [**1-KK**].

This PI is analogous to the Faraday instability initially observed in hydrodynamics under the external forced modulation of the vertical position of an open fluid tank [37]. However, since it is generated by the geometric properties (i.e., the parabolic index profile of a GRIN fiber) rather than by external forces, we have dubbed this novel frequency conversion “geometric parametric instability” or GPI. Indeed, GPI sidebands are phase-matched by the dynamic refractive-index grating, self-induced via the Kerr effect from the periodic oscillations of the beam intensity owing to self-imaging properties of GRIN MMF.

Note that GPI is fundamentally different from all other known types of instabilities: it requires space-time coupling hence propagation of a large number of modes. Moreover, it can be generated regardless the sign of dispersion, while a standard MI leading to temporal breakup of the CW into a set of multimode solitons can take place only in anomalous dispersion regime.

The wave-vectors of pump k_P, and of the GPI Stokes k_S and anti-Stokes k_A sidebands are expected to satisfy the quasi-phase-matching (QPM) condition $2k_P - k_S - k_A = -2\pi h/\xi$, where $h = 1, 2, 3, ...$ The self-imaging period reads as $\xi = \pi\rho/ 2\Delta$, where ρ is the fiber core radius and Δ is the relative refractive index difference. If we limit the frequency dependence of the refractive index to the contribution of chromatic dispersion at the pump wavelength (κ"), the generated GPI sidebands are detuned from the pump by a discrete set of resonant frequency offsets f_h, which satisfy the condition $(2\pi f_h)^2 = 2\pi h/(\xi\kappa'')$, considering as observed in the experiment that the resonant frequencies depend only weakly upon the quasi-CW beam intensity. With a standard GRIN MMF with a ρ = 26 µm, n_{co} = 1.470, n_{cl} = 1.457, and κ'' = 16.55 × 10^{-27} s^2m^{-1} at the pump wavelength of 1064 nm, Δ = 8.8 × 10^{-3}, so that the self-imaging period is ξ = 0.615 mm. These values lead us to analytically predict an extremely large frequency detuning for the first resonant sideband, namely $f_1 = f_m \simeq$ 125 THz.

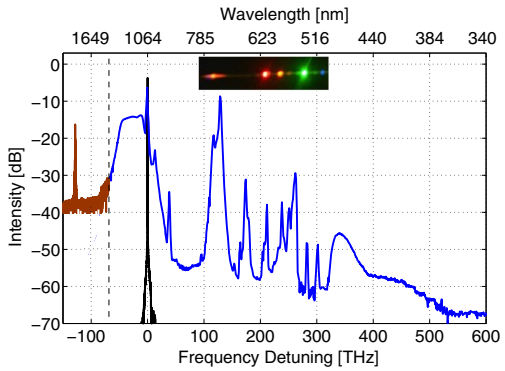

Fig.14 Experimental spectra obtained in 6m-long GRIN MMF with 50 kW of input power $P_{p\text{-}p}$. Inset: photographic image of the visible part of the spectrum dispersed by a diffraction grating. (black curve) Input pump spectrum. Reproduced from [**1-KK**].

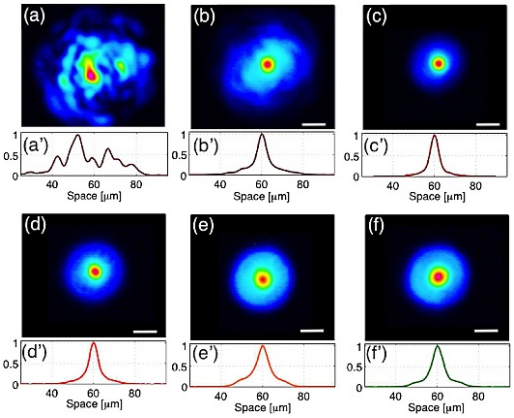

Fig.15 Experimental 2D output spatial shapes (intensity in linear scale) and corresponding beam profiles (normalized intensity) versus x (y=0) at 1064 nm for an input power (a, a') $P_{p\text{-}p}$=0.06 kW and (b, b') $P_{p\text{-}p}$=50 kW, as well as, at first four-orders anti-Stokes sidebands at (c, c') 750, (d, d') 650, (e,e') 600, and (f, f') 550 nm, and for $P_{p\text{-}p}$=50kW. Scale bar: 10 µm. Reproduced from [**1-KK**].

This theoretical prediction agrees well with my original experiment (123.5 THz), in which I used a 6m-long standard GRIN MMF with 52.1 µm core diameter and 0.205 NA. I pumped the fiber with an amplified Nd:YAG microchip laser, delivering 900 ps pulses at 1064 nm with the repetition rate of 30 kHz. The polarized Gaussian pump beam was focused at the input face of the fiber with a FWHMI diameter of 35 µm, which was close to the value of the fiber core diameter resulting in excitation of a large number of guided modes thanks to the presence of unavoidable linear mode coupling. Figure 14 shows an example of the experimental spectrum observed at the input peak power P_{pp}= 50 kW. My results clearly demonstrate that GPI permits the conversion of a NIR laser directly into a remarkable broad spectral range, spanning visible and infrared wavelengths, by means of a single resonant parametric nonlinear effect that occurs in the normal dispersion regime. I also observed that the presence of a strong space-time coupling led to the unexpected recovery of spatial coherence at the pump beam as the power grows above a certain threshold, and the transfer of spatial coherence across the entire range of GPI sidebands, which are carried by a well-defined and stable bell-shaped spatial profile. This

is displayed in Fig.15 presenting the beam profile at the fiber output measured at different wavelengths. Such a spatial self-organization effect has been later called Kerr beam self-cleaning.

Supercontinuum generation

Figure 16 shows the spectral evolution as a function of pump power measured in the 12m-long standard GRIN MMF pumped, as previously, by sub-nanosecond microchip laser at 1064nm [**2-KK**]. As we can see when the pump power grows larger, the initially generated GPI sidebands merge into a broadband supercontinuum (SC) as a result of the interplay of the Kerr effect and stimulated Raman scattering (SRS). I found that for peak powers above 35 kW, the SCG takes an unusual flat shape in the IR part of the spectrum down to around 700 nm in the visible domain.

In the next step, we studied the development of the SC along the MMF by the cut-back method, which permits us to better analyze the competition between the GPI and SRS. We noticed that the GPI and SRS provide the major contributions to the spectral broadening, but their effects occur over different length scales. In addition, we observed that in the very first meter of propagation, the GPI sidebands are generated with the strong first-order anti-Stokes peak at about 730 nm. After a few meters of propagation, the Raman effect comes into play, causing a gradual spectral extension toward the IR side of the spectrum: the resulting pump depletion in turn inhibits further GPI frequency conversion, in favor of SRS, which from then becomes a main effect responsible for spectral broadening. The comparison of the SC intensity profiles obtained for 12 m and 30 m long GRIN MMF, as illustrated in Fig. 17, clearly shows that the isolated GPI sidebands in the visible domain are much better discernible for MMF lengths of about 12 m or shorter. Whereas SC is dominated by the SRS for MMF lengths above a few tens of meters, and this allows for spectrum extension into the MIR up to 2500 nm. Such a broad SC is remarkable, when considering the large linear absorption of the MMF in the MIR. We also observed that for fiber longer than 20 m the IR spectrum is no longer flat but exhibits significant spectral ripples: the first three Raman Stokes sidebands between 1100 and 1350 nm can be easily identified.

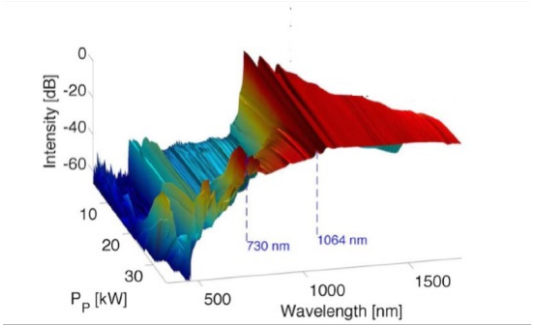

Fig.16 Experimental SC spectra as a function of pump peak power P_p. Fiber length: 12 m. Reproduced from [**2-KK**].

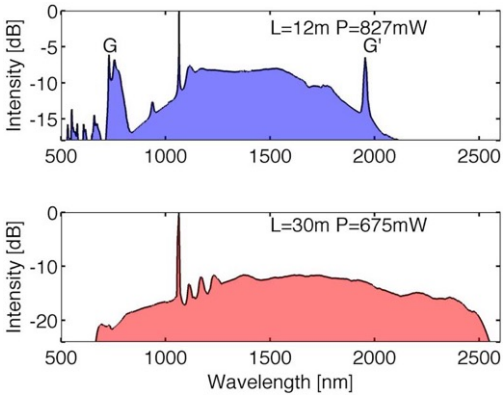

Fig.17 Comparison of SC intensity profiles with 12 m (top) and 30 m (bottom) of GRIN MMF. Reproduced from [**2-KK**].

Moreover, as shown in Fig. 18, we demonstrated that the generated SC is not only spectrally flat or spans more than two octaves, but most interestingly it is essentially carried by the same high-quality bell-shaped beam profile, which remains across all wavelengths very close to the beam waist of the fundamental mode. Figure 18 reports the results obtained for 30m long fiber

where the main mechanism for generating the NIR side of the SC is the Raman effect, which also privileges bell-shaped beams [14]. However, similar results were observed in the visible domain, as well as at the pump wavelength for the short fiber lengths, which is well before the Raman scattering threshold.

Finally, we experimentally analyzed the spectro-temporal structure of the generated SC radiation, as reported in Fig. 19. This was achieved by measuring the fiber output light dispersed by a diffraction grating and detected by photodiodes of 12 GHz bandwidth connected to a 20 GHz oscilloscope. Our spectrogram revealed the presence of a deep temporal modulation within the flat portion of the NIR SC spectrum. In fact, Fig. 19 shows that the largest Raman frequency shift comes from the highest input peak power which, in turn, leads to the strongest pump pulse depletion at the MMF output. As a consequence, the different power values of the temporal profile of the input pump pulse are transposed into different wavelength shifts. The relatively short, 6 m, MMF length could also permit us to clearly observe the temporal envelopes of the separate GPI sidebands reveling their significant, temporal compression up to ten times the pulse duration of the input pulse: the temporal envelope of the sideband G at 730 nm, was measured to be of 130 ps which is seven times shorter than that of the pump.

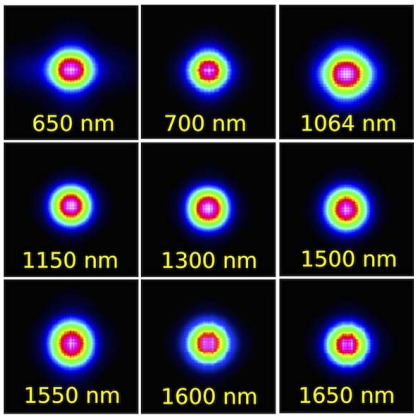

Fig.18 Far-field patterns at the fiber output measured by using different bandpass filters (10 nm bandwidth) and for 1.4 W input average power. Fiber length, 30 m. Reproduced from [**2-KK**].

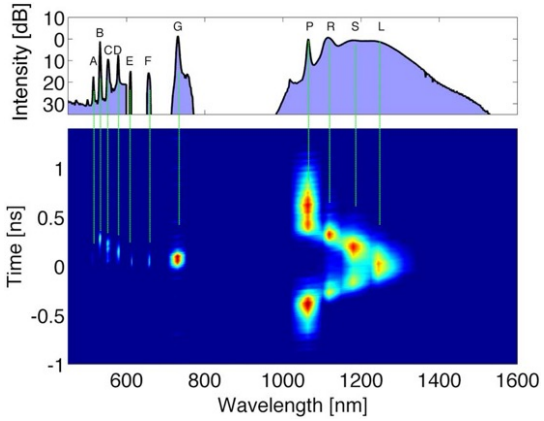

Fig.19 Spectrum (top) and spectro-temporal characterization (bottom) of SC at the fiber output. Fiber length: 6 m. Reproduced from [**2-KK**].

Second Harmonic Generation

We have also studied the spatiotemporal beam reshaping occurring through the co-existence in the same multimode fiber of quadratic and cubic nonlinear responses. Although silica fibers have mainly a cubic nonlinear susceptibility, the presence of dopants can provide a local microscopic quadratic nonlinear susceptibility that can be strongly exacerbated to produce a strong second-harmonic generation (SHG). One of the possible methods to enhance such quadratic nonlinear response in silica optical fiber is known as optical poling, and it is essentially based on a quite long exposure to a strong laser beam.

In the optical poling process, an intense fundamental frequency (FF) pump generates a photo-induced charge distribution, giving rise to a permanent modulated quadratic nonlinearity, whose period automatically satisfies the quasi-phase matching (QPM) between the FF and the second harmonic (SH) waves [38,39]. The estimated QPM period is 48 μm for a FF wavelength of 1064 nm. However, the efficiency of the optical poling process is essentially driven by the FF pump intensity. In GRIN MMF, an intensity reaches periodic maxima equally spaced by a sub-

millimetric self-imaging period. For standard 52/125 GRIN MMF the self-imaging period is of 0.615 mm. As a consequence, the amplitude of the quadratic nonlinearity exhibits an additional modulation with the self-imaging period, and the written quadratic susceptibility has then a double periodicity. Therefore, differently from what has been reported in poled single-mode fibers, the SHG in GRIN MMF manifests completely new spectral and spatial dynamics that we have unveiled and demonstrated experimentally in [**5-KK**].

We used initially poled 6m long standard GRIN MMF that we pumped with 900 ps microchip laser at 1064nm exciting a large number of modes. Figure 20 presents a collection of spectra measured along the fiber for an injected peak power of 37.5 kW. Our experimental results show how the SH builds up from the first tens of centimeters of propagation. We clearly see that as the infrared pump spectrum starts to broaden through the action of Raman effect, a series of closely spaced sharp sidebands grow around the most intense SH peak at 532 nm. A total of eight peaks are observed at the following wavelengths: 476 nm, 488 nm, 501 nm, 515 nm, 532 nm, 552 nm, 576 nm, and 606 nm. Those discrete sidebands around the SH originate from the discussed above additional slow periodic modulation of quadratic nonlinearity induced by multimode nature of pump beam propagation in GRIN fiber (i.e. self-imaging) that leads to the following modified QPM condition for poled MM-GRIN fibers:

$$\Delta\beta - q\frac{2\pi}{\Lambda_S} = \beta(2\omega) - 2\beta(\omega) - \frac{2\pi}{\Lambda} - q\frac{2\pi}{\Lambda_S} = 0,$$

where $\beta(\omega)$ and $\beta(2\omega)$ are the linear propagation constant of the FF and SH plane wave, respectively. Λ is the QPM period that satisfies the condition $\Delta\beta = \beta(2\omega) - 2\beta(\omega) - \frac{2\pi}{\Lambda} = 0$. In optical poling this condition is satisfied generally in a narrow band at the pump wavelength and at its SH. Λ_S is the self-imaging period, that is 0.615 mm for the used fiber and it acts as a second long period grating. While, q = 0, ±1, ±2, ... is associated with each different harmonic of the self-imaging period. In presence of a broadband pump, the SHG may then assume the form of multiple peaks.

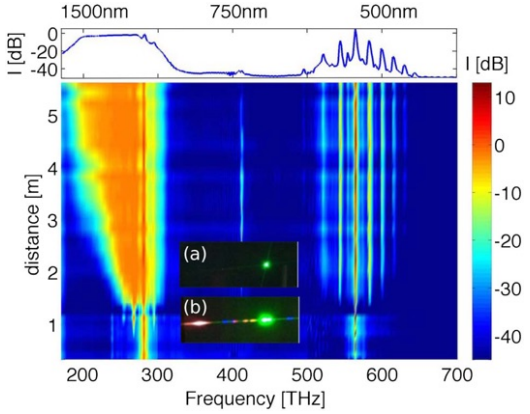

Fig.20 Spectra measured along the poled MM-GRIN fiber by the cut-back method (in the absence of GPI); The insets show a photo of the output beam (a) without and (b) with GPI. Reproduced from [**5-KK**].

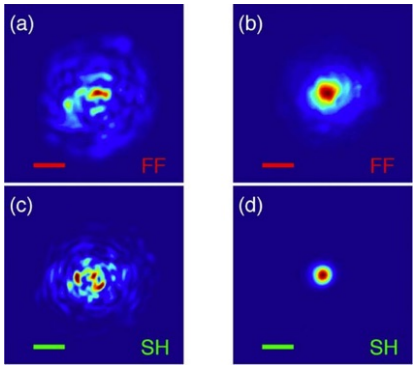

Fig.21 Measured FF and SH beam shapes at the output of a 2 m long poled MM-GRIN fiber. The pump peak powers are: (a, c) 0.94 kW and (b, d) 39 kW. Scale bar: 10 μm. Reproduced from [**5-KK**].

Interestingly, we also observed [**5-KK**] that similar to the case of GPI sidebands induced in the unpoled GRIN MMF, in the poled GRIN fiber the mutual interaction between the FF and its SH strongly affects the spatial distribution of guided light for both colors at the fiber output. An example of the spatial profiles of SHG at the output of a 2 m long GRIN MMF is presented in Fig. 21. Panels (a) and (c) of Fig.21show the fundamental pump and the resulting SH beam

with a relatively low input pump power of 0.94 kW. Panels (b) and (d) of Fig.21 show instead the case of an input pump at 39 kW. When increasing the pump power, both FF and SH output beams evolve from disordered multimode speckles into two bell-shaped beams. While the mechanism for pump beam reshaping can be ascribed to that of previously discussed Kerr beam self-cleaning, the fact that the SH beam also acquires a bell shape was unexpected. In fact, propagation at the SH is much more multimodal than at the FF and moreover the SH is too weak to sustain its own Kerr-induced beam cleaning. Indeed, SH beam cleaning has been achieved via mutual nonlinear coupling with the self-cleaned FF.

Spatial and spectral shaping tailored by refractive index profile of multimode fibers

I have also investigated a role played by the refractive index profile for shaping spatiotemporal dynamics of nonlinear wave propagation in MMFs, as reported in [**10-KK**].

It is well known that any deviation of the refractive index profile of a GRIN MMF from the ideal parabolic shape has direct consequences on the spacing among propagation constants of its modes. I have showed that this simple consideration impacts the Kerr-induced beam self-cleaning, and more strikingly it has dramatic consequences on the mode selection properties of parametric sidebands generated in GRIN MMF.

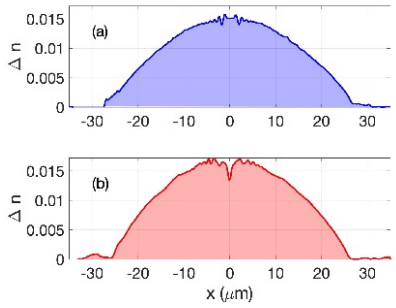

Fig.22 Measured refractive index profiles of the fiber with parabolic index profile (a) without and (b) with a dip on the top. Reproduced from [**10-KK**].

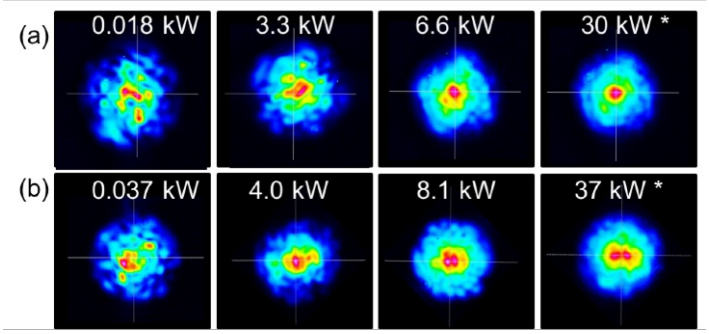

Fig.23 Experimental output 2D near-field shapes (normalized intensity to the local maximum) as a function of input guided power measured at 1064 nm. Panels (a) and (b) show the results obtained for slightly different input conditions. Asterisk (*): results for the power at which frequency conversion into sidebands was also observed. Fiber length: 10 m. Reproduced from [**10-KK**].

In this work, I have used a standard GRIN MMF featuring a local depression in the parabolic index profile. Its measured refractive index profile is illustrated in panel (b) of Fig. 22. For ease of comparison panel (a) of Fig. 22 presents the "ideal" case measured for the fiber used in the previously discussed works. A central index dip may appear in the deposition process, owing to the volatilization of silica and dopants in the innermost layers. This effect is usually unwanted, and it can be circumvented by increasing the concentration of the more volatile dopant. However, as it will be demonstrated it may in fact be exploited to inspire new ways of shaping the spatial and spectral domains of multimode light waves.

At first, I investigated the influence of a relatively small localized depression in the central part of the fiber index profile on the dynamics of Kerr beam self-cleaning. As reported in panel (a) of Fig. 23, in spite of the presence of such a dip, the evolution of the multimode beam toward a bell-shaped spatial pattern could still occur. However, quite remarkably (when considering that the dip is only a minor modification to the index profile of the fiber) the threshold power required to observe the effect was six times larger than in the case of a GRIN MMF with an ideal parabolic index profile. Moreover, when slightly adjusting the input excitation conditions,

we could also observe the self-organization toward a spatial shape that bears strong resemblance to mode $HG_{0,1}$, as it is shown in panel (b) in Fig. 23. Note that similar odd-parity beam shapes were also experimentally observed when using the ideal GRIN fibers in [20].

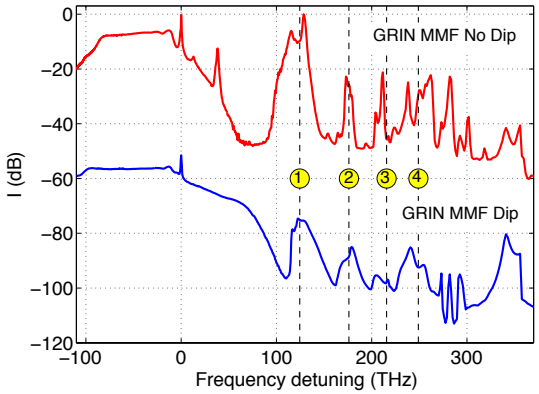

Fig.24 Experimental spectra obtained from GRIN MMF without (top, red curve) and with (bottom, blue curve) a central dip in the refractive index profile. The input guided power was 36 kW. The vertical dashed lines indicate the analytically calculated sideband frequencies. The blue spectrum was down-shifted by 50 dB for better visualization. Fiber length: 10 m. Reproduced from [**10-KK**].

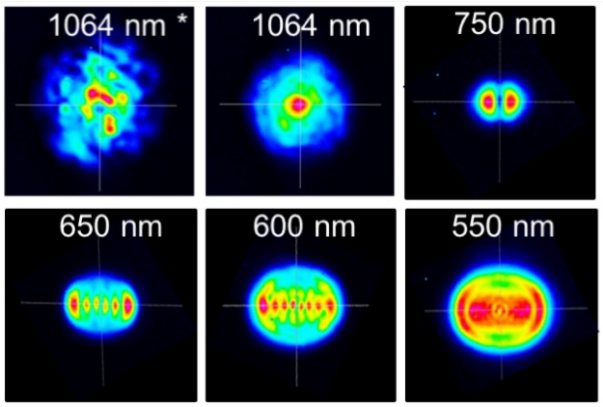

Fig.25 Experimental output 2D near-field shapes (normalized intensity to local maximum) of a series of selected spectral components corresponding to the first four-orders anti-Stokes parametric sidebands, measured from GRIN MMF with a dip in the index profile at 36 kW. Asterisk (*): near-field at 1064 nm in the linear regime. Fiber length: 10 m. Reproduced from [**10-KK**].

Next, I have studied the impact of the fiber index profile modification on the generation of parametric sidebands. Figure 24 compares the experimental optical spectra obtained in the two GRIN MMFs with (blue curve) and without (red curve) the dip, for the same input guided peak power of P_{pp}=36 kW. As we can see, with the fiber with a dip in the index profile, the frequency positions of far-detuned anti-Stokes sidebands obey well the values predicted by the theory of GPI (vertical dashed lines in Fig.24). However, the index perturbation leads to a broadening of sideband spectral bandwidths. Note that although the two fibers had the same diameter and numerical aperture, in order to establish a fair comparison of the spectral positions of sidebands, one would need a precise knowledge of their opto-geometric parameters at the pump wavelength. The dynamics and resolution of our spectrum analyzers were also not sufficient to fully resolve any possible difference in sideband positions. On the other hand, my experiments demonstrate that the presence of a refractive index dip has a strong impact on the conversion efficiency. The GRIN fiber with a dip led to much lower (reduced by more than 20 dB) conversion efficiencies with respect to the values observed with the ideal GRIN fiber. Moreover, and most importantly, the experiments clearly demonstrate that differently from the case of ideal parabolic index profile, here only the pump beam at 1064 nm exhibits a spatial distribution with a bell-shaped profile. As displayed in Fig.25, the generated sidebands are carried by high-order odd parity modes: the larger the order of the peak, the higher the order of the associated spatial mode. These sidebands are generated by quasi-phase matching (QPM) via the dynamic grating resulting from the Kerr effect and pump self-imaging.

However, as mentioned above the presence of a refractive index dip modifies the mode propagation constants, which disrupts their regular spacing, hence the exact periodicity of the collective beam oscillations. Indeed, perturbation theory predicts that a dip in the refractive index leads to a shift in the mode propagation constants. Because of their shift, modes exhibit a slightly different beating period, and as a result, different modes get out of step instead of breathing together in unison. The presence of a dip principally affects low order modes with an intensity peak at the center of the fiber core, while only weakly the modes with a zero in the

core center. Such a break in the oscillation synchronism among fundamental and higher-order modes spoils then the QPM between the pump and sidebands strongly reducing its efficiency as a mechanism for sideband generation.

Moreover, as well observed in the experiment, the sideband generation mechanism is no longer GPI with bell-shaped beams over all spectral range, but intermodal modal-four-wave mixing (IMFWM) with sidebands carried by higher-order transverse modes. Note that for an ideal GRIN fiber, GPI and IMFWM can be considered as two equivalent approaches in which the sidebands are generated at the same spectral positions [40].

Spatiotemporal dynamics of beam propagation in non-standard multimode optical fibers

We have also investigated if the similar spatiotemporal beam reshaping can be observed in MMFs beyond the previously used standard commercially available GRIN MMFs, namely in multimode photonic crystal fibers (MM PCF) and multimode soft glass optical fibers.

Beam cleaning and supercontinuum generation in quasi-parabolic-index MM PCF

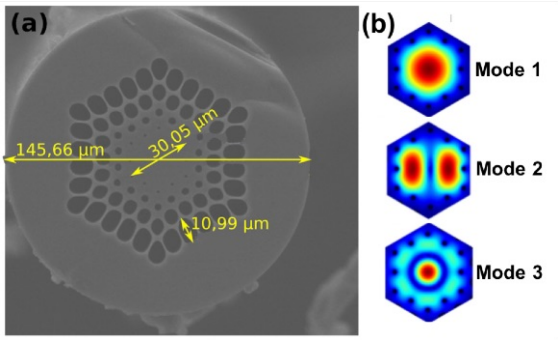

Fig.26 (a) Image of the microstructure MMF from a scanning electron microscope; (b) numerically calculated intensity of the first three guided modes computed at 1064 nm. Reproduced from [**7-KK**].

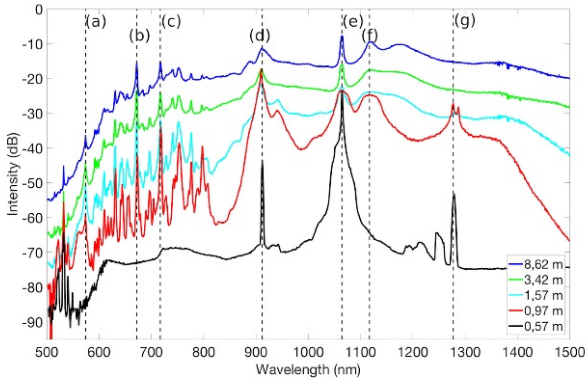

Fig.27 Output spectra for different fiber lengths at input peak power of 120 kW. Reproduced from [**7-KK**].

We studied experimentally the dynamics of the beam self-cleaning, as well as, of the supercontinuum generation in MM PCF, whose transverse structure strongly differs from that of a standard weakly guiding GRIN MMF. We demonstrated in [**7-KK**] that unlike what happens in standard GRIN MMFs, in MM PCF the quality of the output beam does not monotonically increase with growing input power owing to the competition between Kerr beam self-cleaning and Raman beam cleanup. We performed these investigations in a specially conceived microstructure MMF based on a hexagonal pure silica core surrounded by three layers of air holes as optical cladding, whose diameters gradually increase with the layer order (see panel (a) of Fig.26). Such a design leads to a gradual decrease of the (azimuthal) average refractive index resulting in an index profile that can be considered as roughly equivalent to that of a standard fiber, with an intermediate index profile between that of a step-index and a parabolic-index profile. The diameter of the inner silica core was of 30.05 µm, while the total diameter of the fiber was of 145.66 µm. By using Comsol Multiphysics software we found 55 solutions for guided modes at 1064 nm, the intensity profile of the first three modes are illustrated in panel (b) of Fig.26.

We used a spatially single-mode picosecond laser source at 1064 nm, delivering pulses of 60

ps with a repetition rate of 20 kHz. In Fig.27, we show the spectral evolution as a function of propagation distance in the fiber for a fixed input peak power of 120 kW. A first nonlinear frequency conversion takes place after 0.57 m, owing to a modal FWM process, with Stokes and anti-Stokes waves at 1277 nm and 912 nm, respectively in agreement with phase-matching condition involving the modes 1 and 3. For fiber lengths beyond 1 m, we can see a strong SRS-induced frequency conversion into the first Stokes wave at 1117 nm. As the fiber length grows larger, we observe a progressive extension towards the near-infrared and visible part of the spectrum. As a result of an interplay of modal FWM and SRS, a broad supercontinuum ranging from 500 nm up to 1800 nm is generated. In the visible side of the spectrum, the most powerful frequency components are located at 717 nm, 672 nm, and 574 nm and are carried by HOMs. Whereas, the infrared part is guided by the fundamental and low order modes.

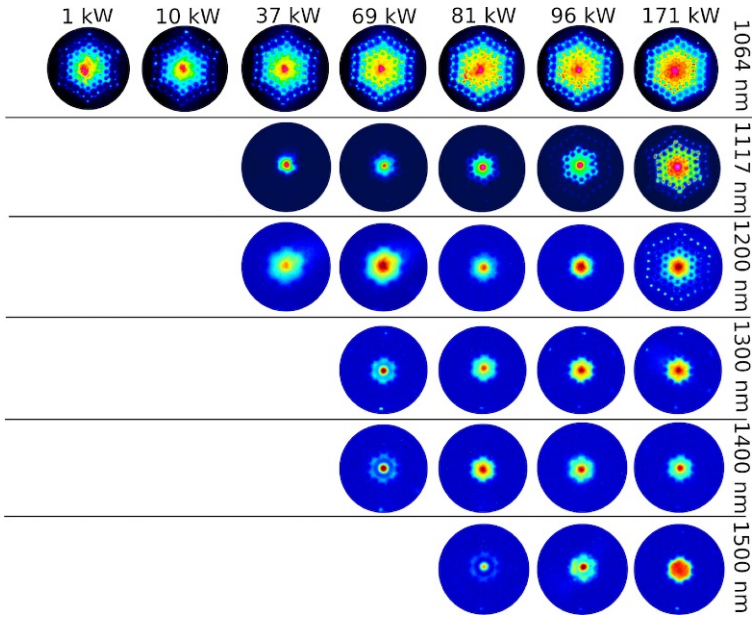

Fig.28 Spatial evolution of the beam profile for different powers and wavelengths. Fiber length: 9 m. Reproduced from [**7-KK**].

Figure 28 presents an overview of beam shape at the output of our 9-m-long MM PCF, at different IR wavelengths and for increasing peak powers. The first row of panels, illustrating the power evolution of the pump beam shape, shows that in our MM PCF we can observe the Kerr self-beam cleaning, however it lasts for a certain range of input powers only, then being quenched by SRS, leading to a multimode speckled pattern at high powers. Indeed, SRS causes a strong energy depletion in the central part of the pump beam, while leaving nearly unchanged its outer part with the major contributions of high-order modes. Note that the first-order Stokes generation (second row of panels in Fig.28) corresponds to the beginning of the pump beam quality degradation.

Similar spatial reshaping happens also for the first-order Stokes wave. Although, initially cleaned through the effect of the Raman beam clean up, the first-order Stokes also experiences decrease of its spatial quality when the second-order Stokes become sufficiently strong depleting the first-order Stokes beam. Moreover, we can observe that the beam shape of spectral components at 1117 nm, 1200 nm, 1300 nm, 1400 nm, and 1500 nm closely resembles a combination of modes 1 and 3 (see panel (b) of Fig.28). In GRIN MMFs, Raman beam cleanup is explained by the dominant modal gain of the fundamental Stokes mode, when compared with the gain of HOMs [14]. Similarly, Raman beam cleanup present in our MM PCF can be explained by the mode selection caused by the difference in overlap integrals that appear in the

exponential gain coefficient of the multimodal Raman scattering process. Indeed, in our fiber, strong Raman conversion results in a progressive transfer of beam brightness toward the infrared side of the spectrum, which is predominantly carried by the lowest order modes.

Spectro-temporal breathing dynamics in GRIN multimode tellurite fibers

Recently, I had started the collaboration with dr hab. M. Klimczak and Prof. R. Buczyński from the University of Warsaw in order to study complex multimode interactions in non-silica MMFs occurring in the femtosecond pulse regime, thus beyond what has been reported so far. We used a multimode fiber with a parabolic index profile that was fabricated in-house in the Institute of Electronics Materials Technology of highly nonlinear tellurite glasses by using the stack and draw technique.

We experimentally demonstrated new interesting dynamics of spectro-temporal pulse breathing observed with increasing pump power while keeping fixed the initial modal excitation conditions [41]. In particular, we observed the presence of a recurrent spectral reshaping manifesting as an increase and a decrease of the frequency conversion efficiency responsible for the generation of the redshifted part of the spectrum. Similar reshaping behavior but obtained by changing modal distribution was also demonstrated in Ref. [42, 43].

Interestingly, we also found that such a recurrent behavior in the spectral domain can be transferred to the temporal domain. The enhancement of the redshifted part of the spectral broadening corresponds to the temporal pulse elongation. Whereas, the further diminution of the redshifted part of the spectrum obtained for the increased power leads instead to the pulse shortening.

Our results have provided indirect evidence of periodic nonlinear mode coupling occurring in graded-index multimode fibers thanks to the modal four-wave-mixing phase-matched via Kerr-induced dynamic index grating.

Beam self-cleaning in nonlinear crystal

Since its first experimental demonstration, in crystalline quartz pumped by a ruby laser by Franken *et al*. back to 1961 [44], SHG has grown to be the most established nonlinear optical effect, with widespread use across laser technologies. The existence of nonlinear self-sustained beams and associated beam reshaping at negative mismatch values was earlier demonstrated for quadratic spatial solitons [45], and, more recently, also by me for polychromatic filaments [46].

In the work discussed in [**12-KK**], we have attempted instead to go further and study if the peculiar effect of spatial beam self-cleaning, understood as a spontaneous recovery of the spatial quality beam from initially fully speckled pattern, can be also observed in the process of SHG.

For this purpose, we used a 30 ps high-energy Q-switched mode-locked Nd:YAG at 1064 nm that first was spatially scrambled by propagation in a short segment of highly multimode optical fiber rod consisting of a glass core of 1 mm in diameter surrounded by a polymer cladding. Next, such a beam was coupled to a KTP (potassium titanyl phosphate) bulk crystal. The phase mismatch for second-harmonic generation (SHG) was varied by tilting the crystal, in order to change the incidence angle between the beam and the crystal facet.

Surprisingly, as presented in Fig.29 our results show that nonlinear beam cleanup may indeed occur in a bulk media with quadratic nonlinearities, albeit in a limited region around phase-

matching, for both signs of the linear phase mismatch. At relatively low energies of the fundamental frequency (FF) beam, that is before any nonlinear spatial beam reshaping occurs, speckled intensity patterns were observed at the output of the KTP crystal. Panels (a), (c), (e) of Fig.29 shows two replicas of the same speckles due to the anisotropy and consequent spatial walk-off in the crystal, which were measured for an input FF beam energy of 0.06 *mJ* and an angle of θ = -1°, θ = 0°, and θ = +1°, respectively. However, as illustrated in panels (b), (d), (f) of Fig.29, at sufficiently high FF beam energies of 0.25 *mJ*, in all three cases, all spots of the FF beam appear to merge into a single beam, sitting on a low-power background. Note that as the SHG gets well out of phase-matching because of crystal rotation, (the crystal angle is rotated by more than θ = 3°), the self-cleaning effect disappears: the output beam is again speckled, which denotes that the beam exhibits a highly spatially multimode content.

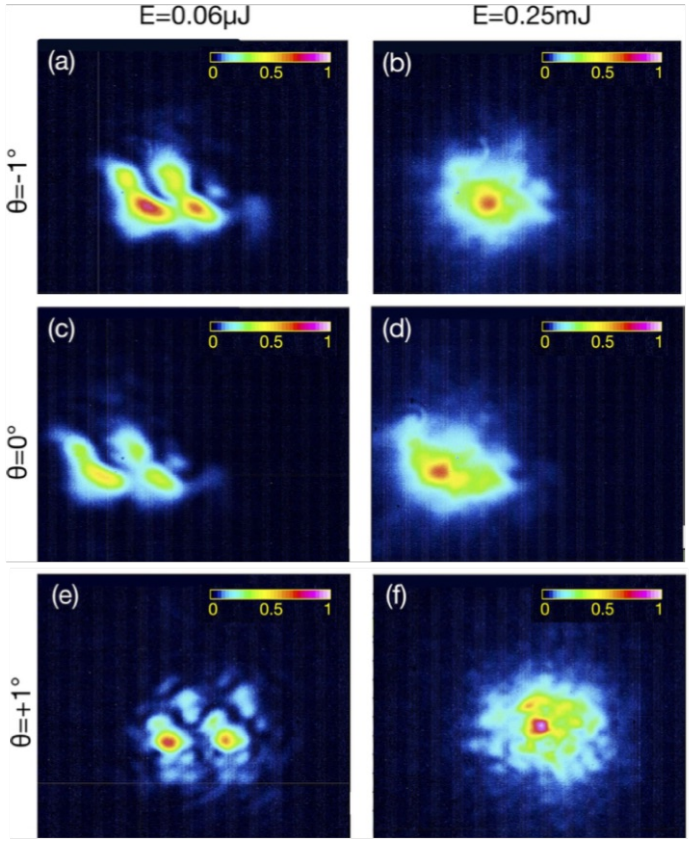

Fig.29 FF beam intensity distribution at the output of the KTP crystal and energy of (a, c, e) 0.06 μJ and (b, d, f) 0.25 *mJ* for an input angle (a, b) θ = -1° (c, d) θ = 0° and (e, f) θ = +1°. Reproduced from [**12-KK**].

To further analyze this novel mechanism of quadratic beam cleaning, we experimentally characterized the nonlinear spatial response of the crystal in the strong conversion regime by using a quasi-plane wave beam. At relatively high FF beam intensities, a significant self-focusing of the FF beam is observed around the phase-matching condition for both positive (focusing) and negative (defocusing) wave vector mismatches. Note that, close to phase-matching of the SHG process, the nonlinear contribution to the propagation of the FF beam can be approximated by a third-order or cubic non-local nonlinear response [47]. This permits us to conjecture a possible connection between the mechanism of self-cleaning in instantaneous Kerr media (*e.g.*, multimode optical fibers), and beam self-cleaning in SHG. This work proves that the beam self-cleaning effect is of more general nature that previously thought. Moreover, because as demonstrated here a beam comprising a large number of spatial wave vectors can indeed increase its brightness, the beam self-cleaning in a quadratic nonlinear bulk media

appears to be of a stronger nature than its Kerr-induced equivalent in MMFs, which usually requires that a predominant excitation of the fundamental beam is present at the input plane.

Applications of GPI and Kerr beam self-cleaning

As already mentioned at the beginning of this research paper cycle, besides their relevance as a test-bed for fundamental research, my findings related to the GPI and Kerr beam self-cleaning have very promising applications in development of novel photonic devices such as spatiotemporal mode-locked fiber lasers and novel broadband light sources [25,48] for nonlinear imaging. Below, I will briefly discuss examples of applications to which I have contributed within the framework of collaboration.

Mid-infrared supercontinuum light source

Fiber laser technology and more specifically, all-fiber-based light sources have made huge progress over the past few decades. Today, SC laser sources based on silica core optical fibers are commercially available, spanning from the visible to the near-infrared spectral region. However, the spectral ranges of short-wave (SW) and middle-wave infrared (MID-IR) remain yet poorly covered by current fiber-based solutions, although these spectral ranges are crucial for numerous important applications, such as for medicine, spectroscopy, imaging, material processing, and remote environmental sensing.

In our work [15], we exploit GPI-based frequency conversion to develop a new all-fiber-based SC laser source emitting high-energy light in the SW/MID-IR, starting from conventional laser sources at 1064 nm. Our all-fiber system is composed of three stages. In the first stage, a 2.3m long segment of 62.5/125 GRIN MMF, pumped by 1 MHz 65 ps pulses at 1064 nm, generates a GPI Stokes at 1870 nm. In the second stage, a 1.5 m long 18/125 thulium-doped fiber amplifier, pumped by an erbium-doped fiber laser at 1560 nm is used to boost the power of such a narrow sideband and obtain an efficient pump for further supercontinuum generation obtained in the third stage with a use of 10m long 9.5/125 InF_3 (fluoro-indate) fiber. This fiber cascade approach allows us to achieve a spatially nearly single-mode broadband light source spanning from 1.7 μm to 3.4 μm with a maximum output power of 75 mW (1 μJ pulse energy).

Nonlinear imaging

Nonlinear imaging also provides an interesting application of nonlinear MMFs. Our work [16] shows that the Kerr beam self-cleaning and its self-induced spatiotemporal reshaping allows for improving performances of nonlinear fluorescence microscopy and endoscopy. We demonstrated that high quality spatial bell-shape beam, induced all-over the entire SC ranging from 700 nm up to 2.4 μm, enables large-band multi-photon fluorescence imaging of biological samples with high spatial resolution approaching its optical limits that is not achievable when exploiting a linear multimode beam propagation. Moreover, we showed that the temporal pulse narrowing associated with the beam self-cleaning thus an increase of the output pulse peak power, has permitted further enhancing the efficiency of nonlinear imaging. Indeed, differently from the case of linear irregular speckled beam, where no image of nucleus in the tested sample of kidney of mouse could be obtained, a clear signature of the nucleus was achieved when imaging with a self-cleaned beam, instead. Note that in both experiments we kept the average power on the sample unchanged. Moreover, the remarkable robustness of Kerr beam self-cleaning phenomenon with respect to fiber perturbations allowed us to achieve high stability of the imaging measurements. Our results then demonstrate that exploiting the nonlinear

multimode dynamics helps enhancing performances of the nonlinear imaging in terms of its resolution, contrast, efficiency and signal-to noise ratio.

Our other work [17] has demonstrated instead that again by exploiting Kerr self-cleaning effect and SCG in GRIN MMFs, it is possible to get rid of the delay lines in the imaging system based on multiplex coherent anti-Stokes Raman Scattering (M-CARS), thus significantly simplifying this set-up, which now can be self-referenced. Note that standard M-CARS systems require an additional delay line to temporally synchronize the pump with the large-band Stokes waves, which complicates and enlarge the system. The SCG causes pump depletion mainly in the center of the beam. However, the beam self-cleaning continuously partially refills the fundamental mode due to the energy transfer from HOMs. Such a pump "refreshment" enables its synchronization within entire spectral range of the Stokes waves without a need additional delay lines. Therefore, although the recovered portion of the pump is quite weak, it was found to be sufficient to obtain quite efficient CARS signal and build the system with performances comparable to those of existing well-known M-CARS systems containing light sources based on SCG in single-mode fibers.

Literature (excluding papers selected to the cycle of my research publications)

[1] D. Gloge, "Optical power ow in multimode fibers," Bell Syst. Tech. J. 51, 1767-1783 (1972).

[2] A. B. Grudinin, E. Dianov, D. Korbkin, A. M. Prokhorov, and D. Khaidarov, "Nonlinear mode coupling in multimode optical fibers; excitation of femtosecond- range stimulated-Raman-scattering solitons," JETP Lett. 47, 356-359 (1988).

[3] Kin S. Chiang, "Stimulated Raman scattering in a multimode optical fiber: self-focusing or mode competition?", Opt. Comm. 95 (1993).

[4] A. Hasegawa, "Self-confinement of multimode optical pulse in a glass fiber," Opt. Lett. 5, 416-417 (1980).

[5] B. Crosignani, and P. D. Porto, "Soliton propagation in multimode optical fibers.", Opt. Lett. 6, 329-330 (1981).

[6] D. Auston, "Transverse mode-locking", IEEE J. Quantum Electron. 4, 420–422 (1968).

[7] A.V. Smith et al, „Mode instability in high power fiber amplifiers", Opt. Exp., 19, 10180 (2011).

[8] L. G. Wright, Z. M. Ziegler, P. M. Lushnicov, Z. Zhu, M. A. Eftekhar, D. N. Christodoulide, F. W. Wise, "Multimode Nonlinear Fiber Optics: Massively Parallel Numerical Solver, Tutorial, and Outlook", IEEE Journal of Selected Topics in Quantum Electronics 24, 5100516, (2018).

[9] W. H. Renninger, F.W. Wise, "Optical solitons in graded-index multimode fibres", Nat. Comm. 4, 1719 (2013).

[10] L. G. Wright, S. Wabnitz, D. N. Chistodoulides, F. W. Wise, „Ultrabroadband dispersive radiation by spatiotemporal oscillation of multimode waves," Phys. Rev. Lett. 115, 223902 (2015).

[11] L. G. Wright, D. N. Christodoulides, F. W. Wise, „Controllable spatiotemporal nonlinear effects in multimode fibres", Nat. Photon. 9, 306 (2015).

[12] S. Buch, G. P. Agrawal, "Soliton stability and trapping in multimode fibers", Opt. Lett. 40, 225 (2015).

[13] Mahalati RN, Askarov D, Wilde J P, and Kahn JM. "Adaptive control of input field to achieve desired output intensity profile in multimode fiber with random mode coupling". Opt. Express 20, 14321-14337 (2012).

[14] N. B. Terry, T. G. Alley, T. H. Russell, „An explanation of SRS beam cleanup in graded-index fibers and the absence of SRS beam cleanup in step-index fibers", Opt. Exp. 15, 17509-17519 (2007).

[15] Y. Leventoux, G. Granger, K. Krupa, T. Mansuryan, M. Fabert, A. Tonello, S. Wabnitz, V. Couderc, and S. Fevrier, "Frequency-Resolved Spatial Beam Mapping in Multimode Fibers: Application to Mid-Infrared Supercontinuum Generation", Optics Letters 46, 3717 (2021).

[16] N. Ould Moussa, T. Mansuryan, Ch.-H. Hage, M. Fabert, K. Krupa, A. Tonello, M. Ferraro, L. Leggio, M. Zitelli, F. Mangini, A. Niang, G. Millot, M. Papi, S. Wabnitz and V. Couderc, "Spatiotemporal beam self-cleaning for high-resolution nonlinear fluorescence imaging with multimode fiber", Scientific Report 11:18240 (2021).

[17] S. Wehbi, T. Mansuryan, K. Krupa, M. Fabert, A. Tonello, M. Zitelli, M. Ferraro, F. Mangini, Y. Sun, S. Vergnole, H. Kano, S. Wabnitz, and V. Couderc, "Continuous spatial self-cleaning in GRIN multimode fiber for self-referenced multiplex CARS imaging", Optics Express 30, 16104 (2022).

[18] K. Baudin, A. Fusaro, K. Krupa, J. Garnier, S. Rica, G. Millot, and A. Picozzi, "Classical Rayleigh-Jeans condensation of light waves: Observation and thermodynamic characterization", Physical Review Letters 125, 244101 (2020).

[19] M. Ferraro, F. Mangini, M. Zitelli, S. Wabnitz, "On spatial beam self-cleaning from the perspective of optical wave thermalization in multimode graded-index fibers, Advances in Physics: X 8, 1-35, 2023

[20] E. Deliancourt, M. Fabert, A. Tonello, K. Krupa, A. Desfarges-Berthelemot, V. Kermene, G. Millot, A. Barthelemy, S. Wabnitz, V. Couderc, „Wavefront shaping for optimized many mode Kerr-beam self-cleaning in graded-index multimode fibers", Optics Express 27, 17311-17321 (2019).

[21] S. Chekhovskoy, O. S. Sidelnikov, A. A. Reduyk, A. M. Rubenchik, O. V. Shtyrina, M. P. Fedoruk, S. K. Turitsyn, E. A. Zlobina, S. I. Kablukov, S. A. Babin, K. Krupa, V. Couderc, A. Tonello, A. Barthélémy, G. Millot, and S. Wabnitz, „Nonlinear waves in multimode fibers", Rozdział 15 w książce "Handbook of Optical Fibers", Springer Nature Singapore Pte Ltd 2018, doi:10.1007/978-981-10-1477-2_15-1

[22] S. Trillo, S. Wabnitz, R. H. Stolen, G. Assanto, C. T. Seaton, and G. I. Stegeman, "Experimental observation of polarization instability in a birefringent optical fiber", Appl. Phys. Lett. 49, 1224 (1986).

[23] Y. Levantoux, G. Granger, K. Krupa, A. Tonello, G. Millot, M. Ferraro, F. Mangini, M. Zitelli, S. Wabnitz, S. Février, and V. Couderc, "3D time-domain beam mapping for studying nonlinear dynamics in multimode optical fibers", Optics Letters 46, 66 (2021).

[24] D. Goldstein, Polarized Light, Revised and Expanded, Optical Engineering Series (CRC Press, 2003).

[25] L. G. Wright, D. Christodoulides, F. W. Wise, "Spatiotemporal mode-locking in multimode fiber lasers", Science 358, 94 (2017).

[26] Z. Eslami, L. Salmela, A. Filipkowski, D. Pysz, M. Klimczak, R. Buczyński, J. M. Dudley, and G. Genty, "Two octave supercontinuum generation in a non-silica graded-index multimode fiber," Nat. Comm. 13, 2126 (2022).

[27] Z. Liu, L. G. Wright, D. N. Christodoulides, F. W. Wise, "Kerr self-cleaning of femtosecond-pulsed beams in graded-index multimode fiber," Opt. Lett. 41, 3675–3678 (2016).

[28] Y. Levantoux, A. Parriaux, O. Sidelnikov, G. Granger, M. Jossent, L. Lavoute, D. Gaponov, M. Fabert, A. Tonello, K. Krupa, A. Desfarges-Berthelemot, V. Kermene, G. Millot, S. Février, S. Wabnitz, and V. Couderc, "Highly efficient few-mode spatial beam self-cleaning at 1.5 μm", Optics Express 28, 14333 (2020).

[29] M. Fabert, M. Săpânțan, K. Krupa, A. Tonello, Y. Leventoux, S. Février, T. Mansuryan, A. Niang, B. Wetzel, G. Millot, S. Wabnitz, and V. Couderc, "Coherent combining of self-cleaned multimode beams", Scientific Reports 10:20481 (2020).

[30] T. Hansson, A. Tonello, T. Mansuryan, F. Mangini, M. Zitelli, M. Ferraro, A. Niang, R. Crescenzi, S. Wabnitz, and V. Couderc, "Nonlinear beam self-imaging and self-focusing dynamics in a GRIN multimode optical fiber: theory and experiments", Optics Express 28, 24005 (2020).

[31] E. V. Podivilov, D. S. Kharenko, V. A. Gonta, K. Krupa, O. S. Sidelnikov, S. Turitsyn, M. P. Fedoruk, S. A. Babin, and S. Wabnitz, „Hydrodynamic 2D Turbulence and Spatial Beam Condensation in Multimode Optical Fibers", Physical Review Letters 122, 103902 (2019).

[32] P. Aschieri, J. Garnier, C. Michel, V. Doya, A. Picozzi, "Condensation and thermalization of classical optical waves in a waveguide", Phys. Rev. A 83, 033838 (2011).

[33] H. Poubeyram, P. Sidorenko, F. O. Wu, N. Bender, L. Wright, D. N. Christodoulides, and F. Wise, "Direct observations of thermalization to a Rayleigh-Jeans distribution in multimode fibers", Nature Physics 18, 685-690 (2022).

[34] F. Mangini, M. Gervaziev, M. Ferraro, D. S. Kharenko, M. Zitelli, Y. Sun, V. Couderc, E. V. Podivilov, S. A. Babin, and S. Wabnitz, "Statistical meachanics of beam self-cleaning in GRIN multimode optical fibers", Optics Express 30, 10850 (2022).

[35] F. O. Wu, A. U. Hassan, D. N. Christodoulides, "Thermodynamic theory of highly multimode nonlinear optical systems", Nat. Phot. 13, 776-782, (2019).

[36] S. Longhi, „Modulational instability and space–time dynamics in nonlinear parabolic-index optical fibers", Opt. Lett. 28, 2363 (2003).

[37] M. Faraday, Phil. Trans. R. Soc. London 121, 299 (1831).

[38] U. Österberg and W. Margulis, "Dye laser pumped by Nd:YAG laser pulses frequency doubled in a glass optical fiber ", Opt. Lett. 11, 516 (1986).

[39] E. Sauvain, J. H. Kyung, and N. M. Lawandy, "Multiphoton micrometer-scale photoetching in silicate-based glasses", Opt. Lett. 20, 243 (1995).

[40] E. Nazemosadat, H. Pourbeyram, and A. Mafi, "Phase matching for spontaneous frequency conversion via four-wave mixing in graded-index multimode optical fibers," J. Opt. Soc. Am. B 33, 144–150 (2016).

[41] T. Karpate, G. Stepniewski, T. Kardas, D. Pysz, R. Kasztelanic, Y. Stepanenko, R. Buczynski, K. Krupa, and M. Klimczak, "Quasi-periodic spectro-temporal pulse breathing in a femtosecond-pumped tellurite graded-index multimode fiber", Optics Express 31, 13269-13278 (2023).

[42] Y. Leventoux, G. Granger, T. Mansuryan, M. Fabert, K. Krupa, A. Tonello, S. Wabnitz, V. Couderc, and S. Février, "0.75-6 μm supercontinuum generation using spatiotemporal nonlinear dynamics in graded index multimode ber," in *Conference on Lasers and Electro-Optics Europe and European Quantum Electronics Conference* (Optica Publishing Group, 2021), paper cj_3_2.

[43] O. Tzang, A. M. Caravaca-Aguirre, K. Wagner, and R. Piestun, "Adaptive wavefront shaping for controlling nonlinear multimode interactions in optical bres," Nat. Photonics 12(6), 368–374 (2018).

[44] P. A. Franken, A. E. Hill, C. W. Peters, G. Weinreich, "Generation of optical harmonics.", Phys. Rev. Lett. 7, 118–119 (1961).

[45] W. E. Torruellas, et al., "Observation of two-dimensional spatial solitary waves in a quadratic medium.", Phys. Rev. Lett. 74, 5036–5039 (1995).

[46] K. Krupa, A. Labruyère, A. Tonello, B. M. Shalaby, V. Couderc, F. Baronio, A. B. Aceves, „Polychromatic filament in quadratic media: spatial and spectral shaping of light in crystals", Optica 2, 1058-1064 (2015).

[47] F. Leo, et al. "Walk-of-induced modulation instability, temporal pattern formation, and frequency comb generation in cavity-enhanced second-harmonic generation.", Phys. Rev. Lett. 116, 033901 (2016).

[48] U. Teğin, E. Kakkava, B. Rahmani, D. Psaltis, C. Moser, "Spatiotemporal self-similar fiber laser", Optica 6, 1412 (2019).

5. Presentation of significant scientific or artistic activity carried out at more than one university, scientific or cultural institution, especially at foreign institutions

After the conferment of the PhD degree I have been working within several research projects, most of them were funded by the French National Research Agency (*fr.* ANR). My research activities have covered various aspects of free-space and guided nonlinear optics involving different complex systems based on second and third order nonlinear susceptibility, as well as, ultrafast dynamics of fiber lasers.

This section describes my the most significant scientific achievements obtained in this period, other than those set out in art. 219 para 1 point 2 of the Act (see section 4). These scientific activities were mainly carried out in two French research institutes, where I worked as a post-doc, namely at the XLIM Institute of the University of Limoges and at the ICB Institute of the

University of Burgundy Franche-Comté. The most recent results I have obtained instead at the Institute of Physical Chemistry Polish Academy of Science, my current affiliation.

In the following my scientific achievements will be discussed being classified according to the research topic:

- **Four-Wave-Mixing in optical fibers for potential application in quantum optics** (XLIM, Université de Limoges)

After being awarded a PhD degree for my research focused on development of new optical methods for microsystem reliability investigation, I joined the XLIM Institute of the University of Limoges (France) in 2010 as a post-doctoral researcher to work in nonlinear optics. In my first research project, I was experimentally exploring the potentiality of frequency conversion nonlinear effects for being used in quantum communication systems. The research was focused on a specific type of Four-Wave-Mixing (FWM) called Bragg-Scattering (BS) FWM as a promising candidate for quantum optical applications thanks to its intrinsic low-noise nature. I built the experimental set-up and investigated the BS-FWM in highly nonlinear fibers by using two independent frequency-shifted-feedback lasers operating in the continuous-wave regime at telecom wavelengths [Kr2012_IJO]. The study was initially performed in strong signal regime [Kr2012_PTL], further extended to photon-counting regime [Kr2012_OE] under various combinations of polarization states of the pumps. The noise limitations arising from spontaneous Raman scattering photons was investigated, as well.

Obtained results were reported in 3 publications and presented at 5 conferences (see sections II.4 and II.7 of attachment *List of scientific or artistic achievements which present a major contribution to the development of a specific discipline*). They were also described in a book chapter of "*Shaping light in Nonlinear Optical Fibers*", S. Boscolo and Ch. Finot (Eds.), Wiley, Inc., 2016, and review paper by N. Akhmediev et al., Optics Express 20, 27212-27219, 2012.

This research was carried out in the framework of the French National Research Agency project (ANR 08-JCJC-0122 PARADHOQS) obtained by dr. Alessandro Tonello from the XLIM Institute of the University of Limoges (France). Thanks to my results the PARADHOQS project was selected among numerous projects financed by ANR between 2008 and 2011, for being presented in the notebook no.9 of ANR: "*Infrastructures matérielles et logicielles*", which was devoted to report recent advances in the field of Communication Systems, High Performance Computing and Future Networks (http://www.agence-nationale-recherche.fr/fileadmin/documents/2016/ANR-Fiches-Cahier-09-Infrastructures-nov-2016.pdf).

Bibliography:

[Kr2012_IJO] K. Krupa, M. Bettenzana, A. Tonello, V. Couderc, P. Di Bin, S. Wabnitz, A. Barthélémy, „Bragg-Scattering Four-Wave-Mixing in nonlinear fibers with intra-cavity frequency-shifted laser pumps", International Journal of Optics, special issue on Nonlinear Fibre-Based Photonic Technologies, v.2012, article ID 263828, 7 pages, Hindawi Publishing Corporation, 2012

[Kr2012_PTL] K. Krupa, M. Bettenzana, A. Tonello, D. Modotto, G. Manili, V. Couderc, P. Di Bin, S. Wabnitz, A. Barthélémy, „Four-Wave-Mixing in nonlinear fiber with two intra-cavity frequency-shifted laser pumps", IEEE Photonics Technology Letters, v.24 (4), 258-260, 2012

[Kr2012_OE] K. Krupa, A. Tonello, V. Kozlov, V. Couderc, P. Di Bin, S. Wabnitz, A. Barthélémy, L. Labonté, S. Tanzilli, „Bragg-Scattering conversion at telecom wavelengths towards the photon counting regime", Optics Express, v.20 (24), 27220-27225, 2012

- **Spatial and spectral light shaping in nonlinear crystals**
  (XLIM, Université de Limoges)

My next research project, carried out at the XLIM Institute, was focused on the study of the spatio-temporal dynamics of beam propagation in different nonlinear crystals: barium β-borate (BBO), potassium titanyl phosphate (KTP), and periodically polarized lithium niobate (PPLN).

It is known that in a quadratic nonlinear crystals, depending on the sign of the phase-mismatching for second harmonic generation (SHG), an optical beam may undergo either self-focusing or self-defocusing effect. However, as I observed in BBO crystal, the nonlinear crystals can also present some cubic nonlinearity, which manifests far from the phase-matching conditions. As an evidence for competing quadratic and cubic contributions, I demonstrated experimentally the existence of multiple self-focusing and self-defocusing regions against the orientation angle (phase-mismatched values). Moreover, I found that there exist a critical angle of BBO orientation for which the beam can travel almost without spatial deformation thanks to the perfect mutual compensation of the quadratic and cubic nonlinearities, remarkably leading to a zero-focusing point [Kr2014]. Such a concept of "zero-focusing" can be potentially used for manipulation of high energy beams.

Another interesting effect that I discovered experimentally in KTP and PPLN crystals, when working in the strong conversion regime between fundamental wave and its second harmonic, was a significant increase of the SHG acceptance bandwidth, well beyond what one can expect from the well-known shape of the *cardinal sine* function. Simultaneous self-focusing effect was also observed being independent of the phase-mismatch sign, hence occurring even in the regime where a beam should normally experience a nonlinear defocusing effect for moderate pump power [Kr2015_Como, Kr2022].

The most silent feature of this strong conversion regime in PPLN crystal was demonstration that those self-confined nonlinear waves are prone to quadratic temporal modulation instability. This has resulted in generation a threefold broadband spectrum over two octaves that remarkably remains self-sustained for both signs of phase mismatch thanks to the effect of light intensity [Kr2015_Optica]. Moreover, by increasing the temperature of the crystal, i.e. changing the phase matching from positive to negative values, it was possible to control the spectrum shape of these polychromatic filament moving from a flat continuum light to a discrete series of sharp and bright bands.

This research has been continued in the framework of two PhD theses that have been defended in December 2021 by Sahar Wehbi "Imagerie multimodal assistée par un champ électrique pulsé" and by Raphaël Jauberteau "Extreme events in quadratic media: application to nonlinear imaging", both supervised by dr. hab. Vincent Couderc. I had a pleasure to participate in this works as a collaborator. Part of the PhD work of Mrs. Wehbi was focused on using the novel polychromatic beam generated in PPLN crystal as a light source for self-referenced Multiplex Coherent Anti-Stokes Raman Scattering (M-CARS) imaging microscopy. Moreover, she further studied the possibility to control the shape of Supercontinuum generated in PPLN by mixing its second and third-order nonlinearities while varying the input pulse duration and the optical beam polarization [Wehbi2021]. Part of the PhD work of Mr. Jauberteau was focused on providing deeper understanding of previously observed spatiotemporal beam reshaping by studying wave-breaking dynamics and extreme events in PPLN and KTP crystals, respectively.

He observed that in PPLN whenever the energy of the picosecond pump reaches a critical level, the second harmonic (SH) beam breaks into multiple filaments. However, surprisingly, such a beam breakup may gradually vanish as the laser intensity grows larger, leading to a spatial reshaping into a smooth and wider SH beam, accompanied by a substantial broadening of its temporal spectrum [Jauberteau2021]. In KTP crystal instead, it was demonstrated the interesting phenomenon of appearance and then disappearance of a spatially localized two beams at a fundamental and second harmonic frequencies with an increase of the pump energy. Although the phase mismatched SHG seems to be the dominant nonlinear process in the early stage of such a twin beam generation, the temporal wave breaking further observed at the fundamental frequency could be responsible for its disappearance at high intensities [Jauberteau2022].

This work was reported in 6 articles including an article published in the top-ranked journal of Optica (IF: 11.104), and presented at 15 conferences including 4 as invited talks. It also resulted in obtaining a patent (see sections II.4, II.7 and III.3 of attachment *List of scientific or artistic achievements which present a major contribution to the development of a specific discipline*).

Bibliography:

[Kr2014] K. Krupa, M. Conforti, F. Baronio, S. Trillo, A. Tonello, V. Couderc, „Zero focusing via competing nonlinearities in BBO crystals", Optics Letters 39, 925-928, 2014

[Kr2015_Como] K. Krupa, R. Fona, A. Tonello, A. Labruyère, B. M. Shalaby, S. Wabnitz, V. Couderc, „Self-increased acceptance bandwidth of second harmonic generation for high-energy light sources", workshop on „Spatiotemporal complexity in nonlinear optics", 31.08.2015-4.09.2015, COMO, Italy, 2015, IEEE, DOI 10.1109/SCNO.2015.7323996

[Kr2015_Optica] K. Krupa, A. Labruyère, A. Tonello, B. M. Shalaby, V. Couderc, F. Baronio, A. B. Aceves, „Polychromatic filament in quadratic media: spatial and spectral shaping of light in crystals", Optica 2, 1058-1064, 2015

[Kr2020] K. Krupa, R. Fona, A. Tonello, A. Labruyère, B. M. Shalaby, S. Wabnitz, F. Baronio, A. B. Aceves, G. Millot, and V. Couderc, "Spatial beam self-cleaning in second-harmonic generation", Scientific Reports 10:7204, 2020

[Wehbi2021] S. Wehbi, T. Mansuryan, R. Jauberteau, A. Tonello, K. Krupa, S. Wabnitz, H. Kano, Ph. Leproux, S. Vergnole, V. Couderc, "Versatile supercontinuum generation by using ki(2) and ki(3) nonlinearities in PPLN crystal for direct multiplex CARS measurement", Proceeding of SPIE 11770, Nonlinear Optics and Applications XII, 1177017, 2021

[Jauberteau2021] R. Jauberteau, S. Wehbi, T. Mansuryan, K. Krupa, F. Baronio, B. Wetzel, A. Tonello, S. Wabnitz, and V. Couderc, "Boosting and Taming Wave Breakup in Second Harmonic Generation", Frontiers in Physics 9, 640025, 2021

[Jauberteau2022] R. Jauberteau, S. Wehbi, T. Mansuryan, A. Tonello, F. Baronio, K. Krupa, B. Wetzel, S. Wabnitz, and V. Couderc, "Twin Spotlight Beam Generation in Quadratic Crystals", Communications Physics 5:197, 1-7, 2022

- **Ultra-long fiber lasers for cryptography application**
  (XLIM, Université de Limoges)

During my stay in the XLIM Institute, I was also participating in the project focused on development of novel way to establish a secure data transmission over long distances. Together

with my colleagues I proposed a new approach to generate an alphabet for secret key exchange between two parties. We demonstrated experimentally how the small variations in the cavity length of an ultra-long fiber laser, hence the variations of its radiofrequency spectrum can be used for this purpose. The test bench for the proof of principle was a laser, working at telecom wavelength, with a cavity composed of two bidirectional 25-km-long fiber segments linking two users: Alice and Bob, where each user could randomly add an extra 1-km-long segment of fiber using an electro-optical switch. As a result, the laser cavity has a random length determined by the combination of users' choices and taking on the values: 50 km (0,0 state), 51 km (0,1 or 1,0 state) and 52 km (1,1 state), and hence, random is also the free spectral range (FSR). The security of key exchange is ensured whenever the two independent random choices lead to the same laser cavity length, that is to the same FSR. Only Alice and Bob, knowing the result of their own random choice, can distinguish the two secure states. This ultra-long fiber laser would open up new perspectives for studying secure communication in non-traditional regimes using a simple protocol and low-cost standard components [Ton2015].

This work was published in the top-ranked journal of Light: Science and Applications of Nature Group (IF: 17.782), and presented at 3 conferences including 1 as an invited talk (see sections II.4 and II.7 of attachment *List of scientific or artistic achievements which present a major contribution to the development of a specific discipline*)

Bibliography:

[Ton2015] A. Tonello, A. Barthélémy, K. Krupa, V. Kermene, A. Desfarges-Berthelemot, B. M. Shalaby, S. Boscolo, S. K. Turitsyn, J. D. Ania-Castañón, „Secret key exchange in ultra-long lasers by radio-frequency spectrum coding", Light: Science & Applications 4, Nature Publishing Group; e276; doi:10.1038/lsa.2015.49, 2015

- **Real-time ultrafast dynamics of fiber lasers**
  (ICB, Université de Bourgogne Franché-Comté and Institute of Physical Chemistry PAS)

In 2016, I moved to the Laboratoire Interdisciplinaire Carnot de Bourgogne (ICB) of the University of Bourgogne Franche-Comté in Dijon (France) to work on ultrafast fiber lasers. I have studied experimentally the complexity of dissipative optical systems exploring their ability for various types of pulse-pulse interactions and dynamic pattern generation. I provided the first direct (real-time) experimental evidence of internal motion within ultrafast soliton pair molecules in a mode-locked fiber laser, thus confirming the existence of such internal dynamics previously anticipated by numerical simulations. By using a dispersive Fourier-transform technique (DFT) I revealed different categories of soliton molecular dynamics. The first one is combined oscillations of both the relative soliton phase and temporal separation between the two bound solitons, along each cavity round-trip, in analogy with the vibrations of a matter diatomic molecule. The second one mainly consists of a sliding relative phase [Kr2017_PRL].

This work was published in top-ranked Physical Review Letters journal (IF 9.161), currently obtaining of 339 citations without self-citations (*according to Scopus*). This article was selected for Editors' Suggestion and presented in APS Physics 10, s64, 13 June 2017, in the section of Synopsis: Coupled Solitons Jiggle Like Molecules. Moreover, these results were independently highlighted and spotted by the Science journal (*Science 357, issue 6346, 2017*) in the sections of Nonlinear optics of Editors' Choice and The Week in Science.

During my stay in ICB institute, I was exploring further the self-organizing ability of dissipative optical solitons, this time in their incoherent regime. I experimentally demonstrated the

existence of a new class of vector dynamics of incoherent dissipative solitons. By using DFT, I revealed several salient features of these dynamics. Both polarization locking and polarization switching of the incoherent soliton were observed, generalizing previous observations made in the coherent case. I showed that transient spectro-temporal ordering can take place among the incoherent pulse. Finally, I also demonstrated that, the vicinity of polarization switching dynamics is prone to the manifestation of explosive instabilities that are with the generation of vector rogue waves [Kr2017_Optica, Gre2017].

This work was published in top-ranked Optica journal (IF 10.644) and a Chapter 6 in the book "Nonlinear Guided Wave Optics", Ed. Stefan Wabnitz, IOP Publishing Ltd. 2017, online ISBN: 978-0-7503-1460-2 (see sections II.4 and II.7 of attachment *List of scientific or artistic achievements which present a major contribution to the development of a specific discipline*).

In December 2019, I moved to the Institute of Physical Chemistry PAS (Poland) where, among others, I has been continuing my research related to real-time characterization of ultrafast pulses. In particular, I has studied the breathing dynamics in an all-normal dispersion all-polarization maintaining Ytterbium-doped fiber laser. I observed breathers, the second frequency, without any change of the fundamental (first) frequency. Beyond the state-of-the-art, I also observed a third frequency, which manifests as a periodic change of breather frequency due to the second Hopf bifurcation. This is the first experimental demonstration of double-Hopf bifurcation in fiber laser that up to now has been studied and predicted in laser systems only theoretically. This interesting observation suggests the high and unexpected complexity of the ytterbium oscillators as dynamical systems, which manifests in the increased number and nature of dimensions of its phase space [Kr2022].

This work has been published in top-ranked Laser&Photonics Review journal (IF 11.0) and presented in 4 conferences (see sections II.4 and II.7 of attachment *List of scientific or artistic achievements which present a major contribution to the development of a specific discipline*).

Bibliography:

[Kr2017_PRL] K. Krupa, K. Nithyanandan, U. Andral, P. Tchofo-Dinda, and Ph. Grelu, "Real-time observation of internal motion within ultrafast dissipative optical soliton molecules.", Physical Review Letters 118, 243901, 2017

[Kr2017_Optica] K. Krupa, K. Nithyanandan, Ph. Grelu, „Vector dynamics of incoherent dissipative optical solitons", Optica 4, 1239-1244, 2017

[Gre2017] P. Grelu, J.-M. Soto-Crespo, K. Krupa, K. Nithyanandan, S. Hamdi, A. Coillet, „Extreme wave dynamics from incoherent dissipative solitons in fiber laser cavities", Chapter 6 in the book "Nonlinear Guided Wave Optics", Ed. Stefan Wabnitz, IOP Publishing Ltd. 2017, online ISBN: 978-0-7503-1460-2

[Kr2022] K. Krupa, T. M. Kardas, and Y. Stepanenko, "Real-time observation of double-Hopf bifurcation in an ultrafast all-PM fiber laser", Laser and Photonics Reviews 2100646, 1-6, 2022

- **Stimulated Raman Scattering in CO_2-filled hollow-core fibers**
  (ICB, Université de Bourgogne Franché-Comté)

In 2019, during my second research stay in the Laboratoire Interdisciplinaire Carnot de Bourgogne (ICB) of the University of Bourgogne Franche-Comté in Dijon, I have been studying spectro-temporal dynamics of Stimulated Raman Scattering in hollow-core fiber filled with CO_2 gas.

The generation of highly efficient multi-octave comb-like spectra through SRS has attracted a lot of attention being widely studied in HC-PCF mostly filled with a hydrogen gas. However, a serious inconvenience here is the high hydrogen permeability of silica, which requires using special actions to protect the fiber from gas leakage. My results demonstrate experimentally that CO_2 gas can provide an interesting new low-pressure solution for the generation of efficient and moreover spectrally very narrow (of around 300MHz) comb-like spectra, which is indeed non-permeable in silica. At only several bars of CO_2 pressure, we generated intense more than one-octave wide Raman spectra in the fiber pumped by a single laser at 1064 nm with a relatively low peak power not exceeding 40 kW [Kr2019_OL].

Moreover, we have studied experimentally and numerically the complexity of the spectro-temporal dynamics of SRS in CO_2-filled HC-PCF. Differently from what has been observed in hydrogen gas, we have found that the manifestation of the self-similarity law can occur also in presence of higher-order Stokes and also anti-Stokes waves in CO_2 gas. Indeed, we have clearly identified the self-similarity process between the pump and the first order Raman Stokes as well as between the first and second order Raman Stokes, leading to the cascading self-similarity process from the moment at which the second order Raman Stokes has a strong power comparable to that of the pump and first Raman Stokes order [Kr2023_JOSAB].

This work has been published in 2 peer-reviewed journals and presented in a CLEO/Europe-EQEC conference (see sections II.4 and II.7 of attachment *List of scientific or artistic achievements which present a major contribution to the development of a specific discipline*).

Bibliography:

[Kr2019_OL] K. Krupa, K. Baudin, A. Parriaux, G. Fanjoux, G. Millot, "Intense stimulated Raman scattering in CO_2-filled holow-core fibers", Optics Letters 44, 5318-5321, 2019

[Kr2023_JOSAB] K. Krupa, A. Parriaux, G. Millot, G. Fanjoux, „Self-similarity in transient stimulated Raman scattering in CO_2-filled holow-core fiber", JOSAB 40, 637-644, 2023

- **Novel method of tuning Four-Wave Mixing sidebands**
  (Institute of Physical Chemistry PAS)

As mentioned above, after moving to Poland in December 2019, I have been continuing my research in the Institute of Physical Chemistry PAS in Warsaw. One of my scientific achievements has been demonstration of a novel physical principle allowing to spectrally tune four-wave mixing (FWM) nonlinear effect.

Spontaneous FWM and stimulated FWM have been investigated over various schemes. However, to date, the wide tunability of the spectral positions of the FWM sidebands has been ensured exclusively by varying the pump wavelength. Differently from the prior art, we developed a new alternative way to spectrally shift the FWM sidebands by varying the chirp parameter of pump pulses in the presence of Self-Phase-Modulation (SPM) while keeping the pump central wavelength fixed. We obtained this effect in a concatenation of two PM optical fibers, a standard PM980 fiber and then a microstructure LMA-PM-5 fiber, in single-pass configuration. The first fiber served for initial SPM generation, followed by FWM induced in the second one. Indeed, the differently stretched pulses when combined with SPM can give rise to two tunable lateral lobes which can act as tunable pumps. When chirp increases (decreases) the redshifted lobe (the closest to the zero-dispersion-wavelength of microstructure fiber)

decreases (increases) in wavelength, and so changing the FWM sideband wavelengths. Importantly, our results demonstrate that this original method allows to obtain the wide tunability of parametric sidebands comparable to the results provided by the state of the art technique of varying the pump wavelength. We validated our method by performing the coherent anti-Stokes Raman scattering (CARS) imaging of simple compounds, such as the polystyrene and the paraffin [Cor2023_OL].

This work has been published in Optic Letters and presented in 2 international conferences (see sections II.4 and II.7 of attachment *List of scientific or artistic achievements which present a major contribution to the development of a specific discipline*).

Bibliography:

[Cor2023_OL] C. Corso, T. Mansuryan, A. Tonello, Y. Arosa, Y. Stepanenko, V. Couderc, K. Krupa, "Tunable four-wave mixing enabled by a self-phase modulation of chirped pulses.", Optic Letters 48, 5531-5534, 2023

6. Presentation of teaching and organizational achievements as well as achievements in popularization of science or art

- **Teaching activities**

2022 **Invited Professor** (University of Limoges, in the framework of Master Erasmus Mundus EMIMEO European project)

Topics: Optoelectronics

Nature / Level: 16h of labworks (in English) / Master

2012 – 2015 **Teaching assistant** (University of Limoges, Faculty of Sciences and Techniques, France)

Topics: Photonics, Optics, Basic Physics, Optical communication systems

Nature / Level: 180h of labworks (in French) / Licence, Master

2004 – 2009 **Teaching assistant** (Warsaw University of Technology, Faculty of Mechatronics, Poland)

Topics: Photonics, Experimental optics, Interferometric methods

Nature: 300h of labworks (in Polish and in English)

Level: Licence, Master, Master ERASMUS MUNDUS, NEMO Summer School "Micro-Optics Measurement & Characterization"

- **Supervising & Co-supervising of post-doctoral researchers**

Supervising:

2020 – 2023 dr. Fatemeh Ghasemi – post-doc at the Institute of Physical Chemistry PAS

Topic: Ultrafast fiber lasers for application to SRS microscopy.

Co-supervising:

2018 dr. Alioune Niang – post-doc at the University of Brescia (Italy)

Topic: Kerr beam self-cleaning in multimode fibers.

- **Co-supervising of PhD students**

2020 – 2024 Mrs. Cassia Corso Silva – PhD student at the Institute of Physical Chemistry PAS

Topic: Widely-tunable all-fiber laser source for Coherent Raman Scattering microscopy.

2020 – 2024 Mr. Mateusz Pielach – PhD student at the Institute of Physical Chemistry PAS

Topic: Novel design and energy scaling in all-fiber ultrafast oscillators.

- **Supervising & Co-supervising of Master students**

Supervising:

2023 Mrs. Yasaman Rahmanimanesh – Master student in cotutelle between Institute of Physical Chemistry PAS and at the Warsaw University of Technology

Topic: Management of temporal dynamics of ultrafast rare earth-doped all polarization, maintaining fiber lasers.

Co-supervising:

2018 Mrs. Graciela Garmendia Castaneda – Master student at the University of Brescia (Italy)

Topic: Polarization evolution in nonlinear optical fibers

2015 Mr. Riccardo Fona – Master student in cotutelle between University of Brescia (Italy) and University of Limoges (France)

Topic: Phase-matching in quadratic crystals for ultra-high peak power: application to spatial beam cleaning.

2012 Mr. Sény Turé – Master student at the University of Limoges (France)

Topic: Four-Wave-Mixing in optical fibers.

2011 Mrs. Michela Bettenzana – Master student in cotutelle between University of Brescia (Italy) and University of Limoges (France)

Topic: Frequency conversion in optical fibers based on Bragg Scattering type of four-wave mixing.

- **Organizational activities**

2022 Co-organizing of the Siegman International School on Lasers, 25 June – 2 July 2022, Checiny, Poland

- **Public engagement and Outreach activities**

2023 Participation in the program of popular science, „Krypton" episode 2, transmitted in TVP Nauka

2018 Interview for the press article published in a local newspaper of Brescia in Italy, *Giornale di Brescia*: "Nuove fibre ottiche per il laser del futuro" (eng. "New optical fibers for new generation laser systems")

2018 Participation in *The European Researchers' Night* at the University of Brescia, Italy; laboratory demonstrations dedicated to general public

2015 Conference about lasers and their applications in the "Turgot" high school in Limoges, France

2009 – 2013 Participation in *The Open Days* for high-school students at the Warsaw University of Technology and University of Limoges

2007 Participation in the exposition *Fascination of The Light* at the Warsaw University of Technology. The goal of this event, addressed mainly to children and young adults, was to popularize the Optics and Photonics by stimulating their curiosity for Science.

7. Apart from information set out in 1-6 above, the applicant may include other information about his/her professional career, which he/she deems important.

- Qualification for University position

  2012 – 2027: « Maître de Conférences » (ang. Assistant Professor) obtained from the French National Council of Universities (fr. CNU), in the section 30: Optical media, and section 63: Electronic, electrical and photonic engineering

  2018 – 2029: « Professore Universitario di II fascia » (ang. Associate Professor) obtained from the Italian Ministry of Education, University and Research (it. MIUR), in the section 09/F1: Electromagnetics

- Participation in the jury of PhD thesis defense

  as a reviewer:

  2024: Mrs. Zahra Eslami, Tampere University, Tampere, Finland

  as a member of jury:

  2021: Mr. Kilian Baudin, Université Bourgogne Franche-Comté, Dijon, France

  2021: Mr. Mesay Addisu Jima, cotutelle between University of Brescia, Brescia, Italy, and University of Limoges, Limoges, France

  2018 : Mr. Carlos Mas Arabi, Université de Lille, Lille, France

- Member of scientific subcommittee of the international conferences

  2024 : subcommittee of S&I11 – Fiber Photonics: Novel Phenomena, Lasers, Systems and Fabrication of the CLEO US

  2023: Multimode Nonlinear Photonics (MNP) Topic of the IEEE Summer Topical Meeting Series (SUM'2023) conference, 17-19 July 2023, Sicily, Italy

  2023: subcommittee of EF - Nonlinear Phenomena, Solitons and Self-Organization of the CLEO/Europe conference

  2021: subcommittee of Nonlinear Guided Waves of the OSA Nonlinear Optics Topical Meeting (NLO)

- Session Chair at the international conferences
- Anonymous reviewer for peer-reviewed international journals (OSA, Elsevier, Science group, Nature group)
- Nov.-Dec. 2021 & Nov. 2022: Invited Professor at the Université de Limoges, Faculty of Science and Technologie, Limoges, France
- External reviewer in the process of evaluation of the Sonata Bis projects of National Science Center (NCN), call 2018 and reviewer in project evaluation of Israel Science Foundation (call 2024)
- Member of the scholarship committee in the Student Internship program *Resonators* of Candela Foundation for talented Polish students in optics and photonics in the call 2022 and 2023

- Major international collaborations

  Dr. V. Couderc, Dr. A. Barthélémy and Dr. A. Tonello from the XLIM Institute of the Université de Limoges (France);

  Prof. G. Millot, Prof. A. Picozzi and Prof. Ph. Grelu from the ICB Institute of the Université de Bourgogne Franche-Comté (France);

  Prof. S. Wabnitz from the University of Roma Sapienza (Italy);

  Prof. D. Modotto, Prof. F. Baronio from the University of Brescia (Italy);

  Prof. A. Aceves from the Southern Methodist University of Dallas (USA);

Podpisano przez/ Signed by:
KATARZYNA
KRUPA
Data/ Date: 31.05.2024 14:05
mSzafir

……..……..……
(Applicant's signature)